uOttawa

L'Université canadienne
Canada's university

FACULTÉ DES ÉTUDES SUPÉRIEURES
ET POSTOCTORALES

uOttawa
L'Université canadienne
Canada's university

FACULTY OF GRADUATE AND
POSDOCTORAL STUDIES

Marc Dostaler
AUTEUR DE LA THÈSE / AUTHOR OF THESIS

M.A.Sc. (Electrical Engineering)
GRADE / DEGREE

School of Information Technology and Engineering
FACULTÉ, ÉCOLE, DÉPARTEMENT / FACULTY, SCHOOL, DEPARTMENT

Multi-Level Random Data Based Correlator Model

TITRE DE LA THÈSE / TITLE OF THESIS

E. Petriu
DIRECTEUR (DIRECTRICE) DE LA THÈSE / THESIS SUPERVISOR

S. Das
CO-DIRECTEUR (CO-DIRECTRICE) DE LA THÈSE / THESIS CO-SUPERVISOR

EXAMINATEURS (EXAMINATRICES) DE LA THÈSE / THESIS EXAMINERS

V. Groza

H. Schwartz

Gary W. Slater
LE DOYEN DE LA FACULTÉ DES ÉTUDES SUPÉRIEURES ET POSTDOCTORALES /
DEAN OF THE FACULTY OF GRADUATE AND POSTDOCORAL STUDIES

Multi-Level Random Data Based Correlator Model

Marc Dostaler

Thesis submitted to the
Faculty of Graduate and Postdoctoral Studies
In partial fulfillment of the requirements
For the degree of Master of Applied Science in Electrical Engineering

School of Information Technology and Engineering
Faculty of Electrical Engineering
University of Ottawa

Your file Votre référence
ISBN: 0-494-11260-3
Our file Notre référence
ISBN: 0-494-11260-3

ABSTRACT

The thesis proposes to develop a virtual prototyping environment (VPE) allowing the study of multi-level random data processing. This VPE allows to experimentally study the effect of different quantization levels and dither signal parameters on the performance of generalized random data correlator architectures.

ACKNOWLEDGEMENTS

I would like to acknowledge the effort and supervision of Dr. Emil Petriu during this research. I would also like to thank Dr Sunil Das, my co-supervisor, as well as my friends, family and coworkers who have helped along the way, financially and emotionally. Their support made this thesis possible.

TABLE OF CONTENTS

LIST OF FIGURES

LIST OF ACRONYMS

A/RD: Analog to Random Data

ADC: Analog to digital converter

ASIC: Application specific integrated circuit

DC: Direct current

DSP: Digital signal processor

MSE: Mean squared error

FPGA: Field programmable gate array

PDF: Probability density function

RD/D: Random Data to Digital

RRQ: Random reference quantization

VPE: Virtual prototyping environment

Chapter 1: Introduction

1.1 Background

The random data correlator architecture is based on the principles of stochastic data processing. The basic concepts, first presented by von Neumann in 1956, provide some advantages in speed and complexity at the expense of accuracy. The general concepts are presented in this introduction, while a more detailed overview of relevant literature is presented in Chapter 2.

1.2 Dithering and Random Data Processing

Random data processing uses low-bit dithered quantization to produce stochastic pulse streams to represent analog variables. Dithered quantization is often used to improve the non-linearity in signal quantization. The dither is used to whiten quantization noise, which then makes it easier to remove via low pass filtering.

Random data processing differs from dithering in that the goal is take advantage of the lower number of bits per quantization level which is used in computation of arithmetic on the stochastic streams. The savings in circuit complexity permit a higher packing density per chip, increasing the amount of functional units that can operate in parallel. The increased savings in cost come at the expense of accuracy, a subject studied in this work.

1.3 Correlation and Correlator Architectures

Correlation is a way of quantifying a measure of similarity between two signals. This feature can be used to match patterns or signals to known models. Applications are found in many kinds of signal processing including communications, optical recognition, and others.

Correlation can be computed in the analog domain using analog components, but in the digital domain there are a few main approaches. General purpose computers can be used to compute correlation functions but are slower than purposefully designed correlators. For higher accuracy and speed, digital signal processing chips (DSPs) can be used as they have specialized computation hardware such as multiple arithmetic units and a specialized instruction set for signal processing applications. The highest speed correlators are purpose built ASIC designs using 1-bit representation, called polarity coincidence correlators.

1.4 Parallel Architecture vs. Serial Architecture

Serial architectures for computation perform operations in an iterative fashion. In digital systems, a clocking signal signals successive calculations in a computation. It will take many cycles to complete. For some types of systems and computations, parallel architectures can perform many calculations in the same cycle, increasing the speed of the output. The cost is increased complexity in the design and an increased resource requirement.

Instruments to calculate correlation functions can take advantage of parallelism to compute all points in the function simultaneously. In practical implementations using standard digital representation this is not always possible as the resources requirements are too great. The resources required for computation using random data is much lower and makes it suitable to the task.

1.5 Thesis Contributions

This thesis work consists of the development of a virtual prototyping environment which was used to study a correlator architecture using generalized random data representation.

Experimental simulations on the effect of reference domain instability in the dither source in random data signal representation show error values similar to those in [27].

The work was inspired by the random data neuron architecture Lichen Zhao presented as requirements for a Master's Thesis in 1998 [44].

1.6 Thesis Organization

This chapter has presented a basic overview of concepts used in the thesis.

Chapter 2 will review current literature review on research on relevant subjects and introduce the theory. Specifically, a study of dithering effects and the choice of dither is presented. Random data based processing is introduced, and a generic parallel correlator architecture is developed.

Chapter 3 explains details of the implementation details of the virtual prototyping environment using the Matlab environment.

Chapter 4 discusses results obtained while studying dithering and generalized random data representation. Errors for signal conversions with and without unstable dithers are presented, as well as the proper operation of the random data based correlator.

Chapter 5 concludes the research and proposes further research.

Chapter 2: Random Data Processing and Correlation

2.1 Review

In a 1956 paper [21], Jon von Neumann proposed the use of computation techniques that mimic biological system by using logic gates to perform algebraic computation with analog variables. This idea of random pulse coding were further investigated in other stochastic computation schemes, such as the noise computer by Poppelbaum and Afuso [28], stochastic computing by Gaines [16] and the Random-Pulse Machine by Ribeiro [29].

The stochastic computation techniques use information contained in streams generated by low-bit dither quantized analog-to-digital converters. The renewed interest in these techniques is in part due to their applications in neural-networking applications and general high packing density in VLSI and FPGA systems for instrumentation is treated further.

In Wannamaker [38], a historical overview of the contributors to the field of dithering is presented, although they have left out some pertinent work by Castanie [7], [8] who was working more towards the stochastic signal processing aspects in the mid to late 1970s. The field of dithered quantization is not new, having been used in video and audio applications since the 1960s, for example Roberts [30] with the use of noise in picture coding for television transmission. The mathematical theory of the effects of dithering has been treated extensively, with much of the early analysis by Widrow [41] and Schuchman [32]. Vanderkooy and Lipshitz studied the properties of non substractive dither in the 1980s in papers for the Journal of Audio Engineering Society [33], [34]. In the late 1980s, Wagdy [35], [36], [37] had also published papers relating to the ideal quantizer's quantization errors in A/D conversion for various dither signals. In Pop [27], the effects of domain instability in the dither used in random-data conversion were studied. Since the mid 90s, other published research in the field of dithered quantization has been done by Carbone doing general analysis and performance measurement in [10], [11], [12]. During the same period, Gray [17] providing Fourier Series proofs about the effects of dither quantization.

Stochastic computing techniques have been studied in an instrumentation and measurement context since the early 1960s. Correlators using stochastic streams appear as early as Jerspers, Chu, Feitweiss' [19] description of the method to compute correlation functions using stochastic pulse streams, and Wolff's et al.'s [42] polarity coincidence correlator. Chronologically following are Berndt's [6] and Chang and Moore's [12] works analysis of stochastic signal based correlators. Castanie also has made contributions to the field of random reference quantization and correlators, from the mid 70s and beyond in [7], [8]. Recently, Petriu [1], [13], [26] used the principles in applications of random pulse based correlators and the study of multi-bit (multi-level) stochastic techniques that can be used in instrumentation.

Since the mid 1980s, some of the research in the field has been due to the lower circuitry cost of arithmetic as compared to traditional digital methods. The high packing density is particularly suitable to VLSI and FPGA technologies. This has proven to be suitable for the implementation of stochastic neural networks in works by Astras [4], Yeap [25], [43], and Zhao [44], where the high level of parallelism can increase the computation speed drastically, at the expense of accuracy.

2.2 Quantization

The study of quantization and the effects obtained by adding a dither signal have been studied for nearly half a century and are still being studied today. The mathematical analyses presented in this section has appeared in papers by Wagdy, Carbone, and Vanderkoy and Lipshitz. A very substantive analysis appears in Wannamaker [38]. The analysis leading to a lower bound on the performance of a quantizer using uniform dither shown here was published in Carbone [10].

Quantization is the mapping of an analog value V to a discrete variable V_q. In uniform quantization, where each quantization step Δ is identical and equal to 1, the quantization equation is

$$V_q = Q(v) = \left\lfloor \frac{v + \Delta/2}{\Delta} \right\rfloor \bullet \Delta \tag{2.1}$$

Where $\lfloor a \rfloor$ is the greatest integer lower than or equal to a. The mapping causes an error in the quantized signal V_q with respect to the analog signal V. This error, denoted e, is defined in (2.2)

$$e = q(v) = \frac{\Delta}{2} - \Delta \left\langle \frac{v + \Delta/2}{\Delta} \right\rangle \tag{2.2}$$

Where $\langle a \rangle = a - \lfloor a \rfloor$ is the fractional part of a. Thus, the process can be modeled as an additive error model.

The input/output characteristics of a L=7 level deadzone-type quantizer and an L=8 level quantizer and their errors are shown in figure 2.1.

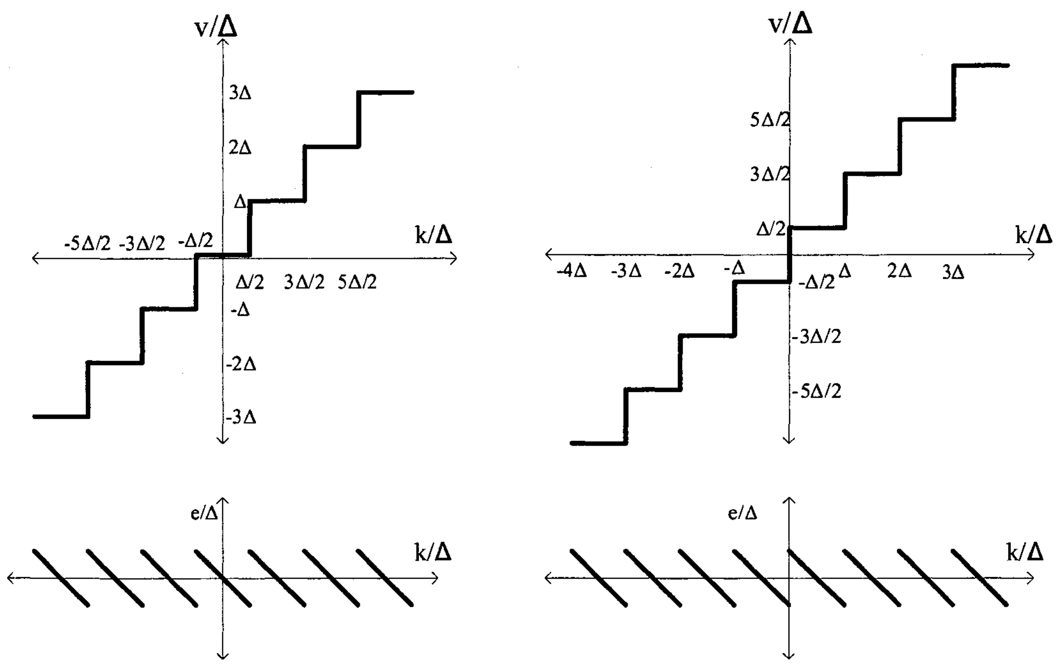

Figure 2.1: Quantizer input/output characteristics

The output symbols of the quantization V_q are k/Δ, and since the uniform quantizer characteristics set Δ to 1, the symbols can be referred to as k. Assuming the signal does not overload the quantizer input, the error function e is periodic with a frequency relationship to k/Δ. The Fourier Series representing the error is:

$$q(v) = \sum_{k=1}^{\infty} \frac{\Delta}{\pi k} (-1)^k \sin(2\pi k \frac{v}{\Delta}) \qquad (2.3)$$

2.3 Dithering and Quantization Error

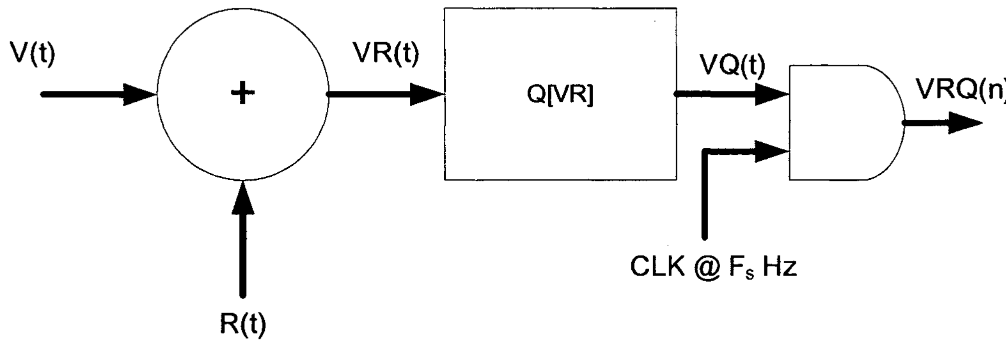

Figure 2.2: Block diagram for dithered quantization

Dithered quantization provides an alternative approach to reducing quantization noise. An analog dither signal R(t) is added to the analog input signal V(t). The resulting signal VR(t) is then repeatedly quantized and clocked so that the discrete dithered signal VRQ(n) is produced. The dither's improvement on the quantization error is observed when a slowly varying dithered signal is quantized and multiple successive samples are examined. If the input variation is slow enough, it can be considered a quasi-stationary process and the expected value y is:

$$\tilde{E}[V] = \lim_{N \to \infty} \frac{1}{N} \sum_{n=0}^{N-1} E[VRQ_q(n)] \qquad (2.4)$$

if the limit exists.

The ideal estimation over an infinite number of samples is E[VRQ] = V. Although the processes under study are quasi-stationary rather than completely stationary, many of the assumptions used in stochastic processing can still be used in analysis. For example, the one Dimensional characteristic function (CF) is defined as

$$\overline{\Phi}_y(u) = \overline{E}[e^{j2\pi uy}] \qquad (2.5)$$

And of its Fourier transform

$$\bar{f}_y(y) = \int_{-\infty}^{\infty} \overline{\Phi}_y(u) e^{-j2\pi uy} du \tag{2.6}$$

when the usual time average is considered. (2.16) represents the well-known amplitude density function (ADF) or probability density function (PDF).

Carbone [10] was reviewed in Zhao [44]. This work, which is derived in part from concepts in Zhao's work, uses the variables from [44] rather than [10]. First, the additive model of the quantization model is depicted in figure 2.3.

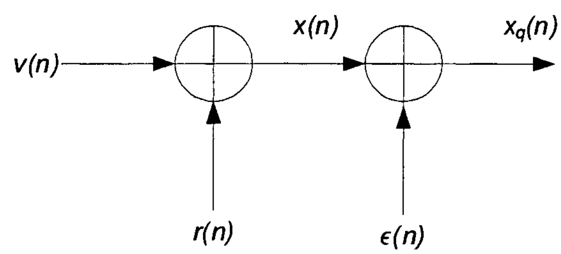

Figure 2.3: Additive model of quantization

The signals *v(n)*, *x(n)*, *r(n)*, and $\epsilon(n)$ are assumed to be continuous-amplitude, discrete-time quasi-stationary processes, while $x_q(n)$ is discrete in both amplitude and time. The dither is assumed independent of the input signal; this means that *r(n)* is independent of *v(k)* for all n and k. Moreover, the one-dimensional statistical description of *r(n)* is assumed to be known. Since uniform dither is of our most interest, the following analysis investigates this aspect further.

A dither with peak-to-peak amplitude R, uniformly distributed, exhibits the following rectangle p.d.f.:

$$f_r(r) = \frac{1}{R} i(s), \qquad S = \left\{ -\frac{R}{2} \le r \le \frac{R}{2} \right\} \tag{2.7}$$

Where i(s) is the indicator function of the set S. Thus, the corresponding CF is given:

$$\overline{\Phi}_r(u) = \sin c(uR) \tag{2.8}$$

In which $\sin c(x) = \lim_{k\to\infty} \sin(\pi k)/(\pi k)$. This distribution can be easily obtained by using a random noise generator.

2.3.1 Effects of dither on Quantization Error

Multiple approaches have been used to find the mean of the quantization error in a dithered signal. Carbone [11] provides a full development including two approaches to the problem, of which only 1 is summarized here. The mean of the quantization error ϵ for a given input v can be written as:

$$\overline{m}_{\varepsilon|w}(v) = \overline{E}[q(v+r)|v] = \int_{-\infty}^{\infty} q(v+r)\bar{f}_r(r)dr \tag{2.9}$$

which can be developed to the following relationship

$$\overline{m}_{\varepsilon|w}(e) = \sum_{k=1}^{\infty} \frac{\Delta}{\pi k}(-1)^{k+1}\overline{\Phi}_r^*\left(\frac{k}{\Delta}\right)\sin\left(\frac{2\pi}{\Delta}ke\right) \tag{2.10}$$

Where v has been substituted by –e due to the periodicity in v with period **Δ** of the sin() function.

$$\overline{m}_{e'|w}(e') = \sum_{k=1}^{\infty} \frac{(-1)^{k+1}}{\pi k}\sin c(2kR')\sin(2\pi ke') \tag{2.11}$$

Where $e' = e/\Delta$, $R' = R/(2\Delta)$, $\varepsilon' = \varepsilon/\Delta$, and $v' = v/\Delta$.

This with some calculations led to the following relationship:

$$\max_{e'}\left[m_{\varepsilon'|v}(e')\right] = \frac{\langle 2R'\rangle}{4R'}\left(1 - \langle 2R'\rangle\right) \tag{2.12}$$

The minimum occurs for R'=(1/2)·n, where n is an integer. This means the quantizer input/output characteristic is no longer a stepwise function, but on the average becomes a straight line, thus realizing infinite resolution.

Error Correlation to the Input

The analysis in Wagdy [35] is used to show the correlation R between the quantizer's input and its error. The development is explained here.

Given the input y and the quantization error e:

$$R = E(y \cdot e) \tag{2.13}$$

Where E is the expectation operator. The correlation function for the k^{th} quantization slot in a bipolar ADC is given by

$$R(k) = \int_{-(k+1/2)\Delta}^{(k+1/2)\Delta} (k-y)y \cdot f_y(y)dy \tag{2.14}$$

Where $f_y(y)$ is the PDF of y. Normalizing with respect to y is achieved by letting Δ=1.

$$R(k) = \int_{-(k+1/2)}^{(k+1/2)} (k-y)y \cdot f_y(y)dy \tag{2.15}$$

The understood dither used in this thesis is uniformly distributed white noise, and its analysis is presented here in addition to that of having no dither.

<u>A. Without dither</u>

The PDF of an pure sinusoid y = Asin(ωt) is given by

$$f_y(y) = \frac{1}{\pi\sqrt{A^2 - y^2}} \tag{2.16}$$

By substitution in the correlation function (2.15), we get

$$R(k) = \int_{k-1/2}^{k+1/2} \frac{(k-y)y}{\pi\sqrt{A^2 - y^2}} \tag{2.17}$$

It can be shown that:

$$R(k) = -\frac{1}{\pi}\left[\phi(x_2) - \phi(x_1)\right] \tag{2.18}$$

$$\phi(x_i) = k\sqrt{A^2 - x_i^{\,2}} + \frac{A^2}{2}\sin^{-1}(x_i) - \frac{x_i}{2}\sqrt{A^2 - x_i^{\,2}} \tag{2.19}$$

$$x_1 = k - \frac{1}{2}, x_2 = k - \frac{1}{2}$$

<u>B with Uniform Dither</u>

By definition, the uniform dither has a rectangular PDF such that

$$f_r(r) = \begin{cases} \dfrac{1}{2c} & ,-c \le r \le c \\ 0 & otherwise \end{cases} \tag{2.20}$$

This dither is added to a sinusoidal input signal with a PDF given in (2.16). Cases where the dither amplitude is smaller or larger than the input amplitude are considered.

1) c<A: When the dither amplitude is smaller than the sinusoid amplitude, the correlation for the kth quantization slot is derived. Using mathematical tables for integration, it can be shown that

$$R(k) = \frac{1}{2\pi}\left[\phi(x_2) - \phi(x_1) - \phi(x_4) + \phi(x_3)\right], k \le A - c - \frac{1}{2} \tag{2.21}$$

Where

$$\phi(i) = -\left(\frac{A^3}{3c}\right)x_i^{\,3}\sin^{-1}x_i + A^2\left(\frac{k}{2c}+1\right)x_i^{\,2}\sin^{-1}x_i - A(k+c)x_i\sin^{-1}x_i$$
$$-A^2\left(\frac{k}{4c}+\frac{1}{2}\right)\sin^{-1}x_i - \left(\frac{A^3}{9c}\right)x_i^{\,2}\sqrt{1-x_i^{\,2}} + A^2\left(\frac{k}{4c}+\frac{1}{2}\right)x_i\sqrt{1-x_i^2} \qquad (2.23)$$
$$-A\left(k+c+\frac{2A^2}{9c}\right)\sqrt{1-x_i^2}$$

$$x_{1,2} = \frac{k \mp \frac{1}{2} + c}{A} \qquad x_{3,4} = \frac{k \mp \frac{1}{2} - c}{A} \qquad (2.24)$$

Also

$$R(k) = \frac{1}{2\pi}\left[\phi(x_2) - \phi(x_1)\right], \qquad (2.25)$$

$$\phi(i) = -\left(\frac{A^3}{3c}\right)x_i^{\,3}\cos^{-1}x_i + A^2\left(\frac{k}{2c}-1\right)x_i^{\,2}\cos^{-1}x_i + A(k-c)x_i\cos^{-1}x_i$$
$$-A^2\left(\frac{k}{4c}-\frac{1}{2}\right)\cos^{-1}x_i - \left(\frac{A^3}{9c}\right)x_i^{\,2}\sqrt{1-x_i^{\,2}} + A^2\left(\frac{k}{4c}-\frac{1}{2}\right)x_i\sqrt{1-x_i^2} \qquad (2.26)$$
$$-A\left(k-c+\frac{2A^2}{9c}\right)\sqrt{1-x_i^2}$$

$$x_{1,2} = \frac{k \mp \frac{1}{2} - c}{A} \qquad (2.27)$$

Which shows that as c increases, the quantization error is less correlated to the quantizer input, an advantage of large amplitude dither.

2) c>A

When the dither amplitude is greater than the sinusoid amplitude, derivations utilizing mathematical tables lead to:

$$R(k) = 0, |k| \le c - A - \frac{1}{2} \qquad (2.28)$$

$$R(k) = \frac{1}{2\pi}\left[\phi(x_2) - \phi(x_1)\right], c - A + \frac{1}{2} \le |k| \le c + A - \frac{1}{2} \qquad (2.29)$$

Where $\Phi(x_i)$, x_1 and x_2 are given by (2.26, 2.27). This again shows that as c increases, |R(k)| decreases.

2.3.2 Quantization Error Amplitude Spectrum

Wagdy [35] also presented an analysis on the spectrum of quantization errors. The analysis section pertinent to uniform dithering is summarized here. The average error at the output of an ADC with a dither d with PDF p(d) added to the input is (2.30), obtained from (2.3)

$$\bar{q}(x) = \int_{-\infty}^{\infty} q(x+d) \cdot p(d)dd \qquad (2.30)$$

which in the frequency domain is

$$\bar{Q}(f) = Q(f) \cdot P(f) \qquad (2.31)$$

Where $\bar{Q}(f)$, *Q(f)* and *P(f)* are the Fourier Transforms of $\bar{q}(x)$, *q(x)* and *p(d)* respectively.

Without dither, the amplitude spectrum is given by

$$|Q(\omega)| = \sum_{n=1}^{\infty} \frac{\Delta}{n} \delta(\omega - n\omega_0) \qquad (2.32)$$

Where $\omega_0 = 2\pi / \Delta$

A uniform dither as described by (2.20) is added to the signal. The Fourier transform of its PDF is

$$P(\omega) = \frac{\sin(\omega c)}{\omega c} \qquad (2.33)$$

Using (2.31), (2.32) and (2.33), we arrive at

$$\left|\overline{Q}(\omega)\right| = \sum_{n=1}^{\infty} \frac{\Delta}{n} \left| \frac{\sin(2\pi nc/\Delta)}{2\pi nc/\Delta} \right| \cdot \delta(\omega - \omega_0) \qquad (2.34)$$

As Wagdy observed, the spectrum of the averaged quantization error can be nullified by choosing an appropriate value for c. This occurs when nc/Δ or 2nc/Δ is an integer, otherwise the spectrum is not nullified.

2.3.3 Dither Signal Characteritics

The dither signal should respect the following conditions from Schuchman [32], that is

1. Have 0 mean
2. Independent of the input signal, having no unwanted correlations
3. Characteristic functions with periodic 0s

Uniform Dither

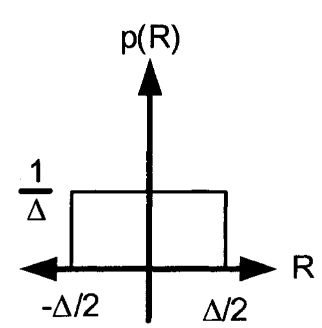

Figure 2.4: PDF of a uniformly distributed dither signal

The simplest dither which satisfies the 3 characteristics consists of uniformly distributed random noise bounded within 1 quantization interval Δ, which is, ranging between –Δ/2 to Δ/2.

Mathematically, the dither function R has a p.d.f. as follows:

$$p(R) = 1/\Delta; -\frac{\Delta}{2} < R < \frac{\Delta}{2} \qquad (2.35)$$
$$p(R) = 0; otherwise$$

From equation (2.34), the dither signal need not be limited to a single quantization interval Δ, but rather that the domain can be over any multiple jΔ where j is an integer.

Reference Domain Instability

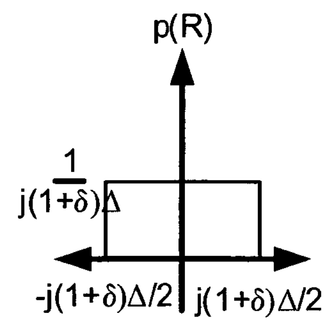

Figure 2.5: PDF of a uniformly distributed dither with domain instability error

Pop [27] studied the effect of domain instability on the random reference quantization error. In practical applications, the dither signal R will have some error δ in its bound c (2.20). The dither function is then

$$f_r(r) = \begin{cases} \frac{1}{2c} & , -c \le r \le c \\ 0 & otherwise \end{cases} \qquad c = j(1+\delta)\frac{1}{2}\Delta \qquad (2.36)$$

The effect of δ is studied experimentally in section 4.2.

2.4 Analog/Random Data Conversion

2.4.1 Generalized Conversion

Analog to random data conversion changes a dithered analog signal into a stochastic stream of leveled pulses. This is achieved by adding a dither signal R and then quantizing the signal and then sampling the signal according to a system sampling rate. Figure [2.2], shown previously, gives the block diagram of the system. The dither signal should respect the dithering conditions previously stated, that is no correlation to the input, have 0 mean, and a characteristic function with periodic 0s.

The signal is then repeatedly quantized to produce VRQ(n)

$$VRQ(n) = k\Delta \quad ,(k - \tfrac{1}{2})\Delta < VR(n \cdot \Delta t) \leq (k + \tfrac{1}{2})\Delta \tag{2.37}$$

In a practical application the quantizer has a limited input domain and an overflow region. Figure 2.5 shows 3 signals from the block diagram in figure 2.2, random data conversion. They are the input to the system V(t) in black, the dithered input VR(t) in red and the quantized and sampled values VRQ(n) in blue. At each time index, the dithered signal VR(t) is quantized using a 3-level deadzone quantizer. The sampled output VRQ(n) is the random data representation of the analog input signal V(t).

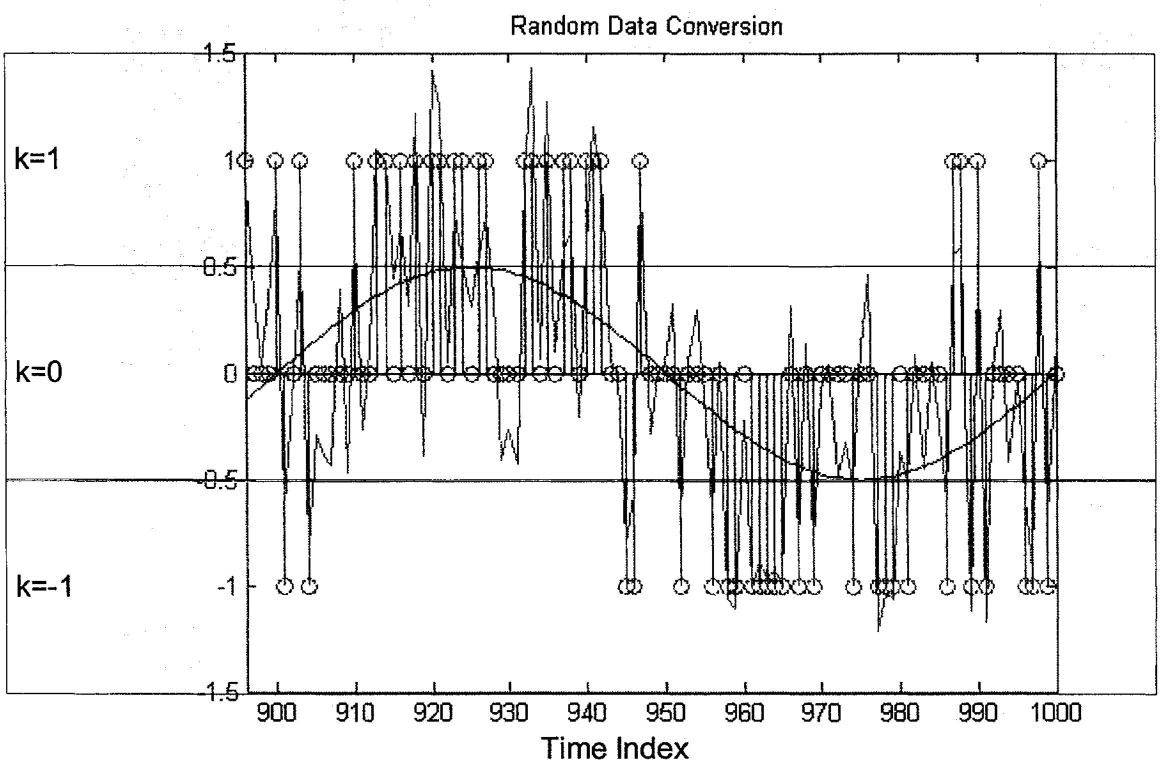

Figure 2.6: Random data conversion

2.4.2 Random Data/Digital Conversion

Gendron and Petriu [24] presented random data to analog conversion as applied to a 1-bit random data signal. The same concept applied to generalized random data representation was shown in [26]. The deterministic component V* of the discrete stochastic signal VRQ(n) can be estimated as the average over a number N_{av} samples. As N_{av} increases, accuracy is improved at the cost of bandwidth of V. The ideal estimate can be computed given infinte samples. Given that β is the offset of V within the quantization interval k, and p[] denoting the probability, the estimation for a 2-level system is found using (2.38) from [26] (Figure 2.7):

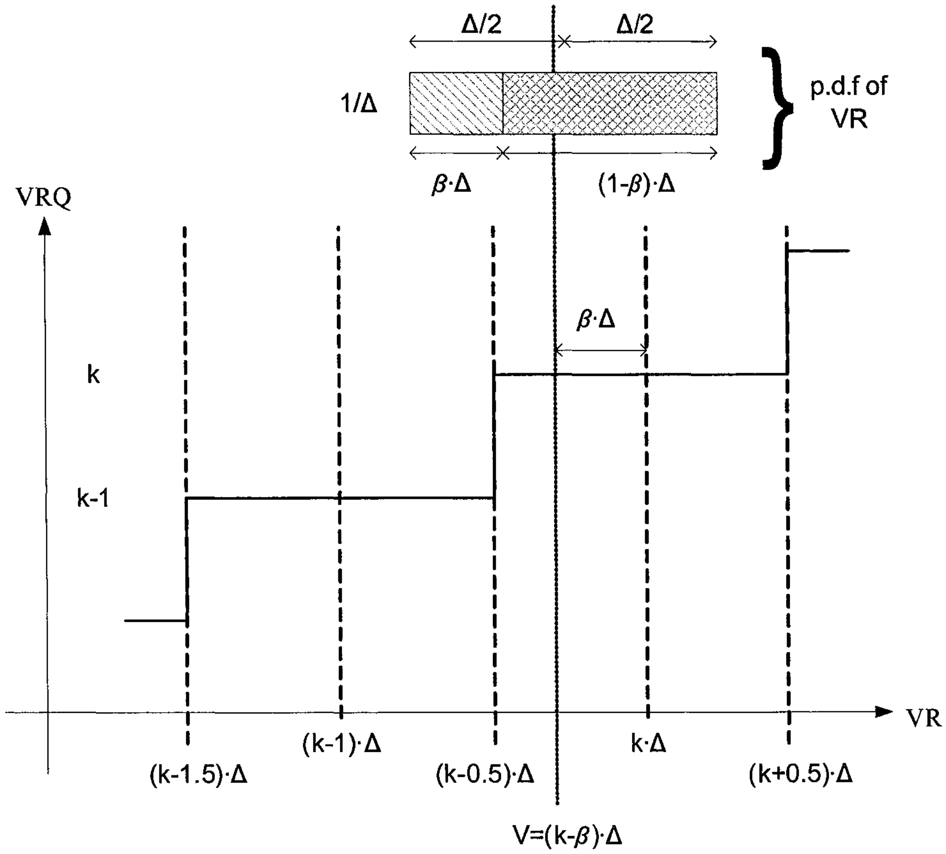

Figure 2.7: Analog/Random Data conversion (adapted from [26])

$$\begin{aligned} E[VRQ] &= (k-1)\bullet p[(k-1.5)\Delta \le VR < (k-0.5)\Delta] \\ &\quad + k\bullet p[(k-0.5)\Delta \le VR < (k+0.5)\Delta] \\ &= (k-1)\bullet \beta + k(1-\beta) = k-\beta \end{aligned} \tag{2.38}$$

The deterministic component of the signal V can be recovered from a limited number of samples from the random data stream VRQ(n) by computing the average over a number of samples N_{av} (2.39).

$$V^*_{Nav}(n) = \frac{1}{Nav}\sum_{n=0}^{Nav-1} VRQ(n) \tag{2.39}$$

The block diagram for this system is shown here in figure 2.8

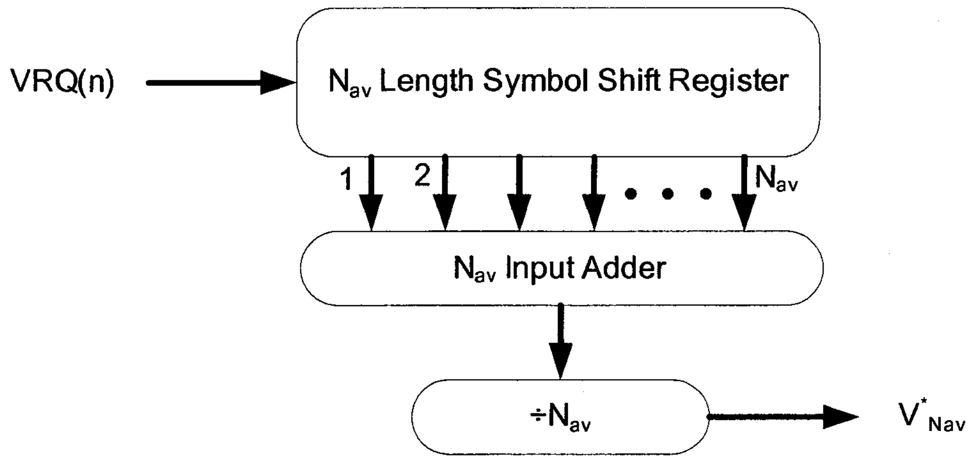

Figure 2.8: Block diagram of Random Data/Digital conversion

The low-pass filtering effect of the averaging algorithm and it is shown in Appendix A.

2.5 Arithmetic

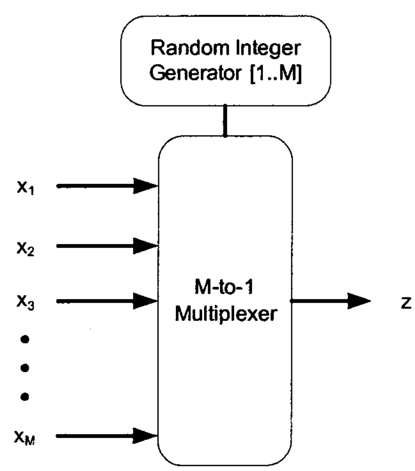

Figure 2.9: Block diagram of random data addition

Arithmetic of stochastic streams is possible by time multiplexing the signals in random order fashion. A stochastic input selector selects one of the available M inputs with uniform probability of 1/M. This scanning is done to remove statistical dependence between the inputs. The resulting output sequence represents $z = (x_1 + x_2 + \ldots + x_M)/M$.

It should be noted that this random data addition is not actually used in the implementation of the correlator because the final integration involves only the stream of product samples (M=1) and not the integration of multiple streams of data samples.

2.6 Multiplication

Multiplication of two unbiased random data streams $VRQ_1(n)$ and $VRQ_2(n)$ is accomplished by multiplying the random data symbols with each other in time. Given that

$$V_{12}(t) = V_1(t) \bullet V_2(t) \tag{2.40}$$

Which, in the random data representation becomes

$$V^*{}_{12}(t) = V_1^*(t) \bullet V_2^*(t) \tag{2.41}$$

The deterministic component of the random pulse representation of this equation $V^*{}_{12}(n)$ can be recovered using the random data/analog conversion algorithm previously discussed.

$$V_{12}^*(n) = \frac{1}{N}\sum_{n=0}^{\infty} VRQ_1(n) \bullet \frac{1}{N}\sum_{n=0}^{\infty} VRQ_2(n) \tag{2.41}$$

$$V_{12}^*(n) = \frac{1}{N}\sum_{n=0}^{\infty} [VRQ_1(n) \bullet VRQ_2(n)] \tag{2.42}$$

The input domain of V_1 being +/-D_{v1}, and the input domain of V_2 being +/-D_{v2}, the output domain is +/-$D_{v1}D_{v2}$. If the number of bits per symbol in V1 is b_{v1} and the number of bits in V2 is b_{v2} then the number of bits required will be at most $b_{v1} + b_{v2}$. In practical applications, the increased output domain of the multiplier requires more levels for the multiplier output. Implementations will need to increase the bits per symbol after each multiplier to accommodate the additional bits per output symbol required.

2.7 Correlation

The random data or stochastic correlators have been studied among others in Berndt [6], Chang [12] and Castanie [8].

2.7.1 Serial Correlator Architecture

Correlation is a measure of degree of similarity between two signals. Mathematically, it is defined as:

$$R_{xy}(d) = \frac{1}{M} \int_{t=-\infty}^{\infty} x(t)y(t-d)dt \tag{2.43}$$

and its form in the discrete domain

$$R_{xy}(k \bullet \Delta t) = \frac{1}{M} \sum_{n=-\infty}^{\infty} x(n \bullet \Delta t) y((n-k) \bullet \Delta t) \tag{2.44}$$

$$R_{xy}(k) = \frac{1}{M} \sum_{n=-\infty}^{\infty} x(n)y(n-k) \tag{2.45}$$

The resulting output function $R_{xy}(k\Delta t)$ has coeffients at high values for some value(s) of $k\Delta t$. This $k\Delta t$ is the amount of delay that must be compensated for in the y signal in order to have the signals realign. Equation (2.45) can be computed in the random data domain as

$$R_{xy}(k) = \frac{1}{M} \sum_{n=-\infty}^{\infty} XRD(n)YRD(n-k) \tag{2.46}$$

which can be realized in the system depicted in figure 2.10.

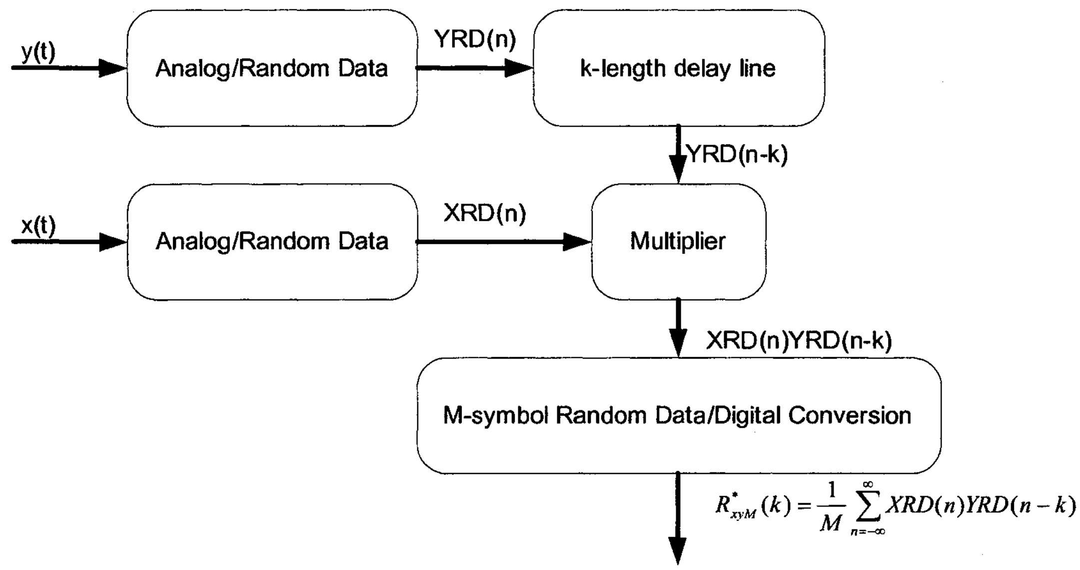

Figure 2.10: Serial correlator architecture using random data representation

In practice, a single correlation point is of little value, and most often the function over a span of indexes is calculated. One way to do this is to use the serial correlator architecture in Figure 2.10 to calculate each point iteratively in a serial fashion. For each correction coefficient k from equation 2.43, the analog signals x(t) and y(t) are converted to random data representation using independent A/RD converters as described in section 2.4.1. The resulting stream YRD(n) is delayed by k samples to give YRD(n-k), and this signal is multiplied with XRD(n). The output is then integrated over N_{av} samples to recover the value of the correlation function at index k. For each index k in the function, the process must be repeated.

The alternative is to implement a parallel architecture where each coefficient k, for each time delay, is calculated simultaneously.

2.7.2 Parallel Correlator Architecture

Using standard digital methods, multipliers of high bit numbers require either a serial algorithm to keep the gate count low, or alternatively have multipliers capable of operating in 1 cycle which have extremely large gate counts. A tradeoff is used in using the serial algorithms that cost time, because the larger multipliers cannot be implemented in parallel on the same chip as they take too many gates.

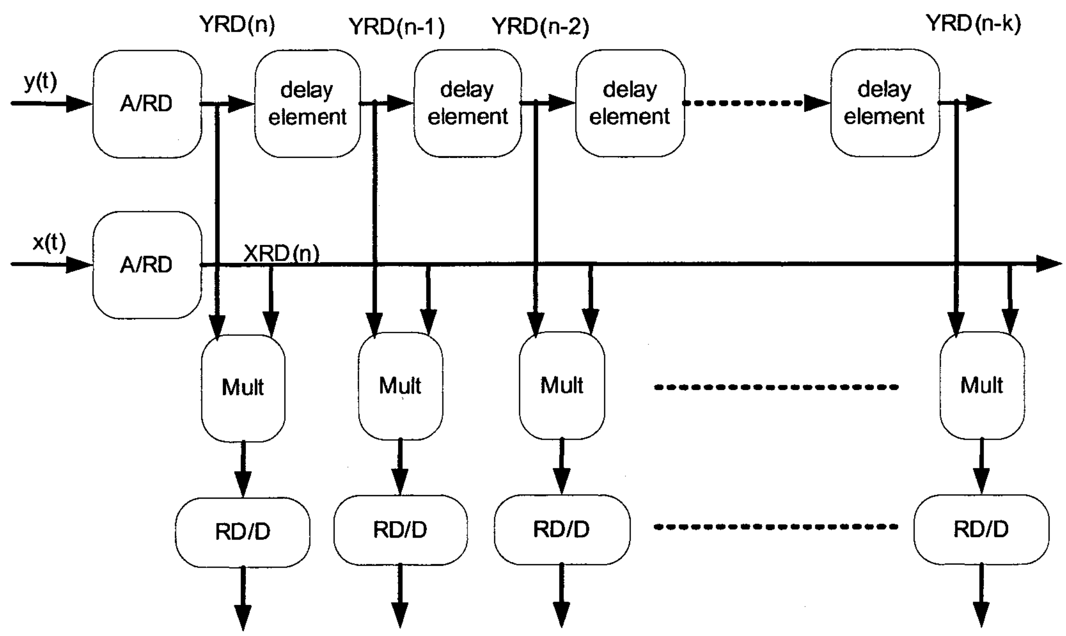

Figure 2.11: Parallel correlator architecture using random data representation

Figure 2.11 shows a conceptual architecture for a parallel correlator. Using random data representation permits the calculation of all the points in parallel, and the results are valid at every clock cycle.

Chapter 3: Virtual Prototyping Environment

3.1 Random Data Correlator Architecture Introduction

The goal is to create a software virtual prototyping environment to study the calculation of the correlation function $R_{xy}(k)$ of two analog signals X(t) and Y(t) using a generalized random data based correlator. The random data representation is used to permit exploiting the high level of parallelism which would be realizable using modern day ASIC and FPGA technologies. The model is built in the Matlab simulation environment, and is operated by means of a graphical user interface.

In the process of designing the random data correlator, the different components were tested. Experiments were designed to study multi-level random data quantization of DC and sinusoid signals; the effects of having a reference domain error δ in the dither source; and finally, multiplication of generalized random data streams. The results appear in chapter 4.

3.2 Analog/Random Data (A/RD) Input Signal Conversion

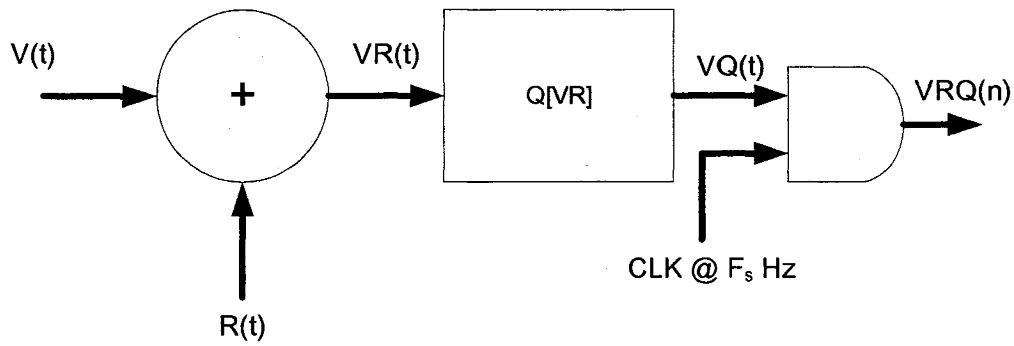

Figure 3.1: Block diagram of Analog/Random Data converter

The generic Analog/Random Data converter shown in Figure 3.1 operates as follows. A dither signal R(t) is added to the analog signal V(t). The resulting signal VR(t) is then quantized to produce an m-bit quantized signal VQ(t). This signal is then converted into its stochastic pulse stream representation by sampling at the system sampling rate, F_s, to generate the random data signal VRQ(n). Independent analog/random data converters must operate on independent dither sources.

3.2.1 Dither Signal Generation

The parameters that control the dither signal domain are their amplitude factors j and the domain instability error δ.

$$f_r(r) = \begin{cases} \dfrac{1}{2c} & ,-c \le r \le c \\ 0 & otherwise \end{cases} \qquad c = j(1+\delta)\frac{1}{2}\Delta \tag{3.1}$$

Where δ is a constant or a random variable. In either case, $|\delta| < 1$.

Uniform Random Dither

The uniform random dither is provided using Matlab's rand() function. This function outputs a pseudorandom sequence of numbers distributed uniformly in the interval [0..1]. The DC bias is removed, providing the dither signal R. The dither signal amplitude is multiplied by the parameter j to increase the dither signal bounds

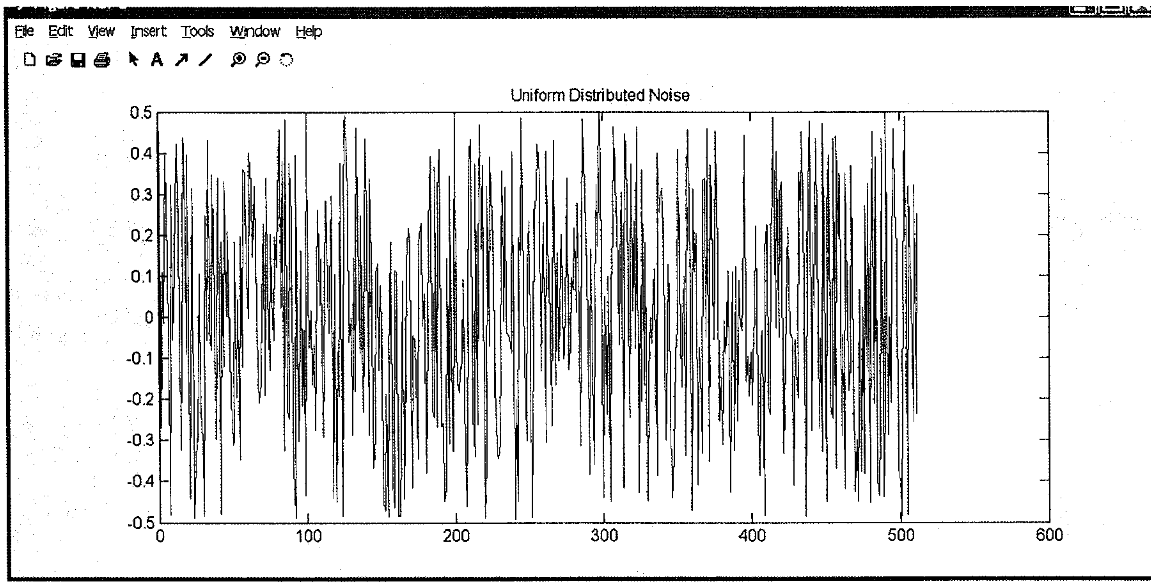

Figure 3.2: Uniformly distributed dither for j = 1

Dither Domain Instability

To study the effect of dither domain instability, the parameter δ can be set to either be a constant value δ or to a random variable uniformly distributed between $\pm\delta$. Experimental results are presented in section 4.

3.3 Random Data Output Symbols

The conversion from analog to random data representation produces a discrete stream of pulses. The quantization characteristic is of the deadzone-type, with a quantization interval centered at the origin. The VPE's quantization characteristic can be set to have no overload region in order to allow the study of an unlimited number of quantization intervals, or the overload region can be modeled to obtain an implementable system . The symbols output are the value of the k^{th} quantization slot as per equation (2.37).

3.4 Random Data/Digital (RD/D) Conversion

In order to take the stochastic data stream VRQ(n) and convert it back to $V_{Nav}*$ the statistical estimation of V, VRQ(n) must be integrated and averaged over a number of samples N_{av}. Mathematically, the function is

$$V_{Nav}^{*}(n) = \frac{1}{Nav} \sum_{n=0}^{Nav-1} VRQ(n) \tag{3.2}$$

This can be calculated serially by implementing the function directly using a shift register and an adder and recalculating $V^{*}_{Nav}(n)$ at each time iteration n. Instead, an iterative moving average algorithm is used, greatly reducing the number of computations required. To accomplish this, the values of VRP(n), VRP(n-Nav) and $V^{*}_{Nav}(n-1)$ are used to calculate $V^{*}_{Nav}(n)$.

$$V_{Nav}^{*}(n) = V_{Nav}^{*}(n-1) + \frac{VRQ(n) - VRQ(n-Nav)}{Nav} \tag{3.3}$$

To simplify this even more, the estimation of $V^*_{Nav}(n)$ is not normalized in the system, removing the need for hardware for division. The simplified equation which is used in system is

$$Nav * V^*_{Nav}(n) = Nav * V^*_{Nav}(n-1) + VRQ(n) - VRQ(n - Nav) \qquad (3.4)$$

And the final normalization, if desired, can be done after all additions in the system. The VPE is designed to use this approach to realistically model the simplest design.

The resulting architecture to compute $V^*_{Nav}(n)$ in figure 3.3 uses a delay line, a substractor and an adder.

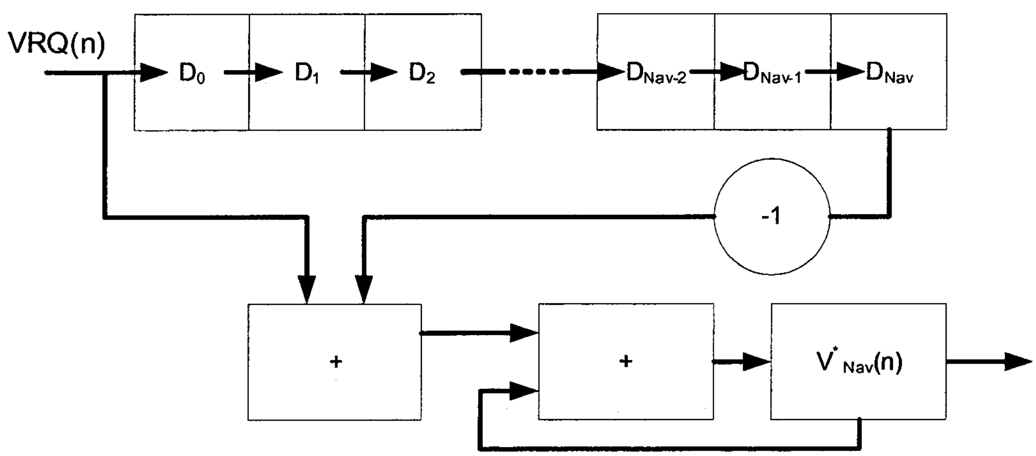

Figure 3.3: Random Data/Digital converter architecture

The subtraction is accomplished by negating the VRQ(n-Nav) and adding it to VRQ(n) using a conventional adder. The result is then added to $V^*_{Nav}(n-1)$ using a feedback loop with a full adder.

The initial conditions set in the VPE for a deadzone quantizer system are such that $V^*_{Nav}(0)$ is 0 and so are all the symbols in the delay line are also 0. In the case of a non-deadzone type quantization, the delay line symbols are initialized such that their average is 0.

3.5 Random Data Multiplier

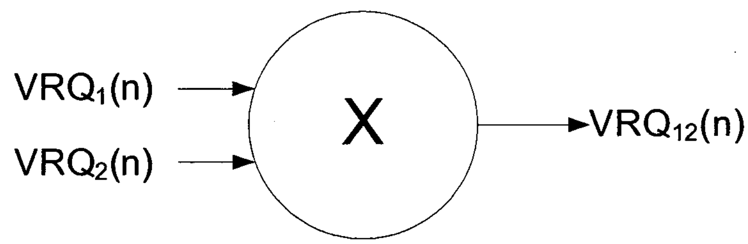

Figure 3.4: Block diagram of random data multiplier

The random data multiplication is done by multiplying the symbols in the random data streams together individually. As the analog inputs $V_1(t)$ and $V_2(t)$ are converted to their random-data representations $VRQ_1(n)$ and $VRQ_2(n)$, the symbol streams are multiplied with each other to output $VRQ_{12}(n)$. $VRQ_{12}(n)$ can then be converted back to a digital representation to obtain the estimation $V^*_{Nav}(n)$ of the multiplication of $V_1(t)$and $V_2(t)$.

Experiments demonstrating the functioning multiplication of generalized random data signals is in section 4.3

3.6 The Correlator Design

3.6.1 Serial Correlator Architecture

A single correlation coefficient at a time delay value $k \cdot \Delta t$ has a value defined as

$$R_{xy}(k \bullet \Delta t) = \frac{1}{N} \sum_{n=0}^{N-1} x(n \bullet \Delta t) \bullet y((n-k) \bullet \Delta t) \quad (3.5)$$

For the purposes of calculation of correlation in the digital domain, the analog time Δt is dropped for clarity.

$$R_{xy}(k) = \frac{1}{N} \sum_{n=0}^{N-1} x(n) \bullet y(n-k) \quad (3.6)$$

This can be computed in random data representation using independent analog/random data converters for the inputs, a k-stage delay line, a random data multiplier and a random data/digital converter. The structure is depicted in figure 3.5.

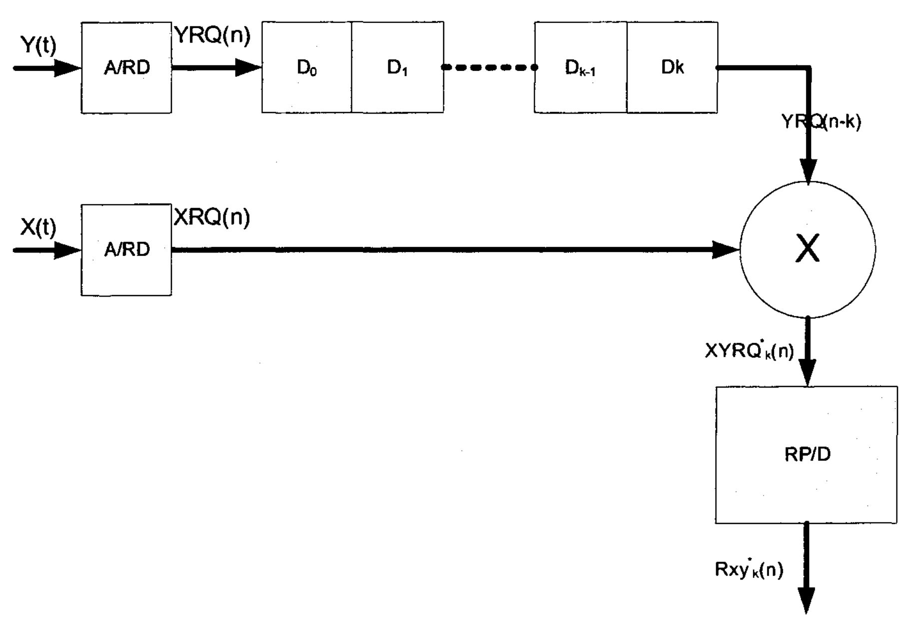

Figure 3.5: Serial random data correlator architecture

The analog X(t) and Y(t) signals are converted to their random data representations XRQ(n) and YRQ(n), respectively, using independent A/RD converters. The stochastic data pulses of the YRQ signal are delayed by feeding them through a k-stage delay line, outputting the delayed signal YRQ(n-k). The two signals XRQ(n) and YRQ(n-k) are then multiplied and the resulting output $XYRQ_k(n) = x(n) \cdot y(n-k)$ is then integrated over a number of samples N. This integration, required from the correlation equation, is accomplished implicitly in the random data/digital conversion as described in section 2.4.1. The resulting output is thus $R_{xy}(k)$, the value of the correlation coefficient at index k.

Using this type of architecture to generate the correlation function requires serial computation of each correlation point. For each index k of the correlation function, the number of delays in the delay line must be increased by one and the process repeated. This architecture requires additional time for the computation of the full correlation function compared to a parallel architecture, but the benefit is that the amount of circuitry required is for the shift registers is significantly reduced.

3.6.2 Parallel Correlator Architecture

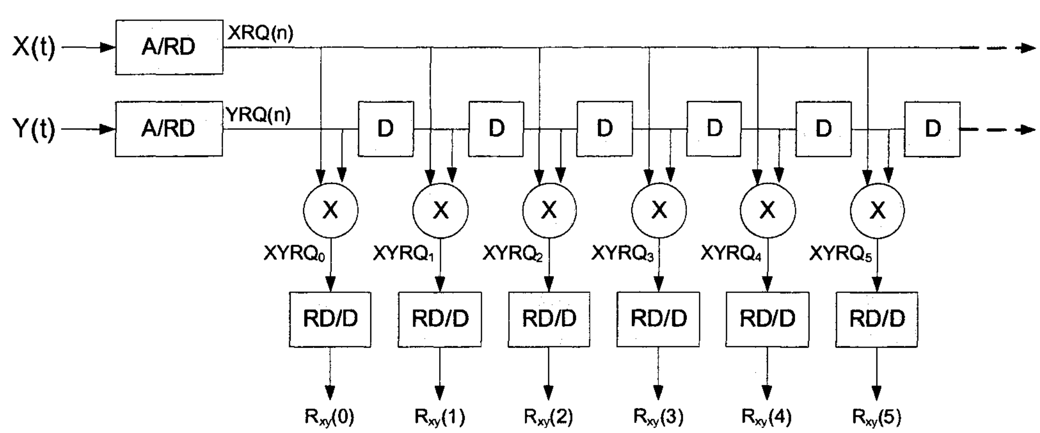

Figure 3.6: Parallel random data correlator architecture

The structure of the 1-point correlator can be taken advantage of to compute multiple correlation points in parallel. A complete correlation function can be calculated by implementing figure 3.6, shown above.

For an M-point correlation, a delay line of length M-1 is required. By multiplying the XRQ(n) signal with the individual outputs of the YRQ delay line elements YRQ(n) to YRQ(n-(M-1)), multiple $XYRQ_k$ streams are generated. The $XYRQ_k$ label is used to identify each pulse stream output from the multipliers, the value k describing how many delays in YRQ were involved in the generation of the pulse stream from the multiplier. Mathematically defined, this interim signal is

$$XYRQ_k(n) = XRQ(n) * YRQ(n-k) \qquad (3.7)$$

Each of these signals is then integrated over Nav samples to compute the correlation coefficients $R_{xy}(k)$. This is done by converting the signals back to digital form using independent RD/D converters.

The simplicity of the circuitry allows for a great number of multipliers to operate in parallel, as opposed to a generic processor where the multiplier often incurs a heavy cost in circuitry. The increased speed in the calculation of the entire correlation function is gained at the cost of the number of registers required which increases by at least 1 + Nav per additional correlation point.

3.6.3 Parallel Correlator Module

The basic building module used in this correlator architecture is a 4-point Random Data correlator. The design is very modular, requiring only to be connected in series in order to compute a correlation function with a larger number of points.

The 4-point random data correlator module is shown below.

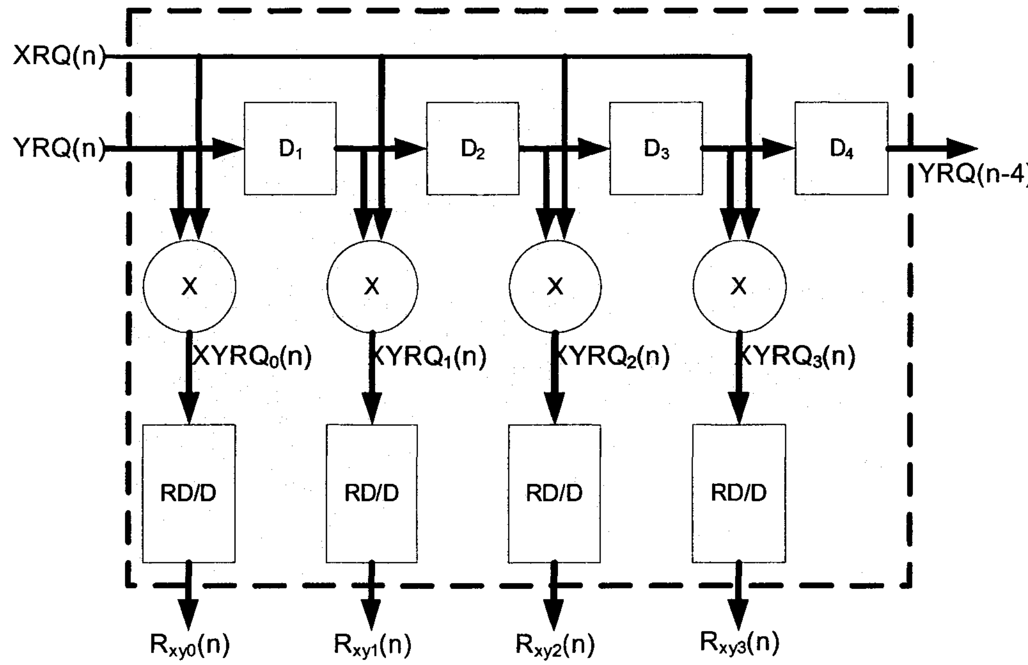

Figure 3.7: 4-point parallel correlator module

The 4-point correlator module operates identically to the generic multi-point architecture but for only 4 points. The inputs of the correlator module are two random data streams XRQ(n) and YRQ(n), and its outputs are the 4 correlation points and the output of the delay line, YRQ(n-4).

The output of the YRQ delay line, YRQ(n-4), can be connected to the YRQ input of the next block, increasing the delay line length and number of correlation points by 4. Concatenating a number B of these blocks leads to a system that calculates a 4*B-point correlation function. The block diagram of such a system with B=3, a 12-point correlation function, is shown below.

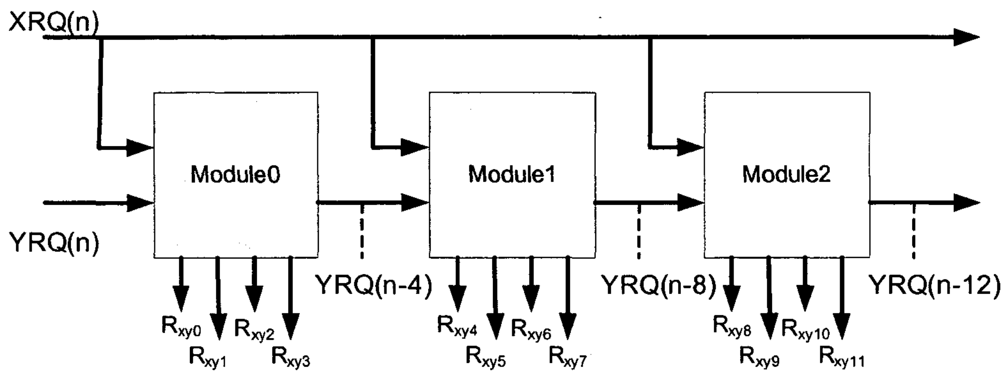

Figure 3.8: Modular parallel correlator architecture

With this arrangement of modules, every operation at every stage can occur on every clock cycle. As such, the correlation results are correct at every cycle in the system.

Chapter 4: Experimental Study of the Generalized Random Reference Quantization Error and the Random Reference Correlator

4.1 Generalization of RRQ by using random noise amplitude domain multiple of Δ (and accepting limited number N of averaged samples)

In section 4.1.1, figures 4.1 to 4.4 show the recovery of an analog DC signal and the mean squared error (MSE) as a function of the window size N_{av} and dither amplitude $j \cdot \Delta$. In terms of dither amplitude domain factors of j, higher j values require a longer average window size N_{av} to attain the same error levels as lower values of j.

Section 4.1.2 studies the recovery of a sinusoidal signal. It is visually obvious that the phase response of the RD/D conversion creates lags in the recovered signal. The error in figure 4.6 is caused not only by the limited number of N_{av} samples used in the recovery, but also by both the attenuation and the phase response due to the causal nature of the RD/D conversion (see Appendix A).

Section 4.1.3 shows error calculations while compensating for the phase difference between the analog and recovered signal gives a better understanding on the source of errors. The error is now due to the amplitude response of the RD/D and to the limited number of average samples N_{av}.

Section 4.1.4 shows experimental results from the quantization of sinusoids of different amplitudes as a function of N_{av} for different dither amplitudes j.

4.1.1 DC Signal Recovery

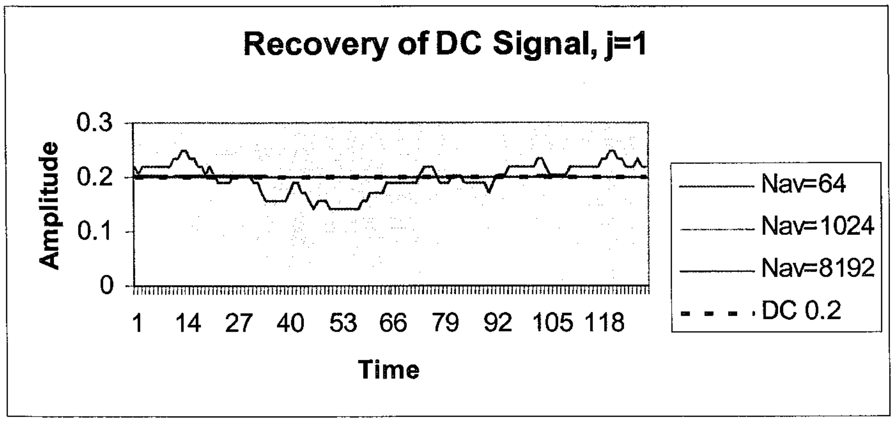

Figure 4.1: Recovery of DC signal for j=1

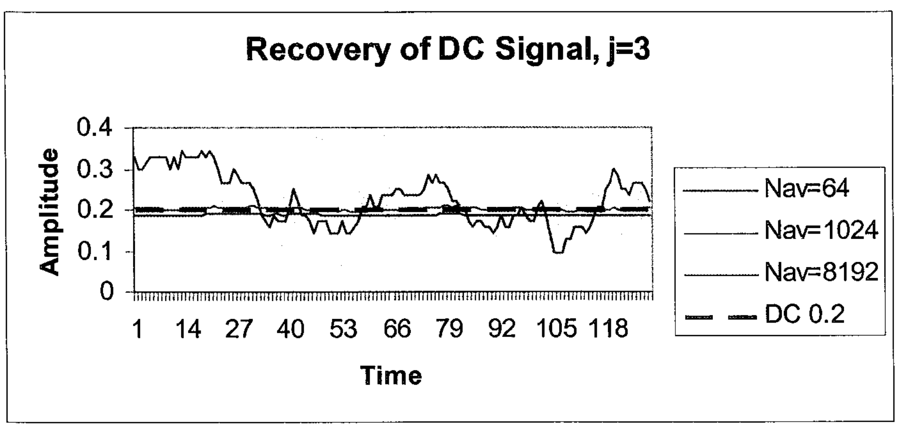

Figure 4.2: Recovery of DC signal for j=3

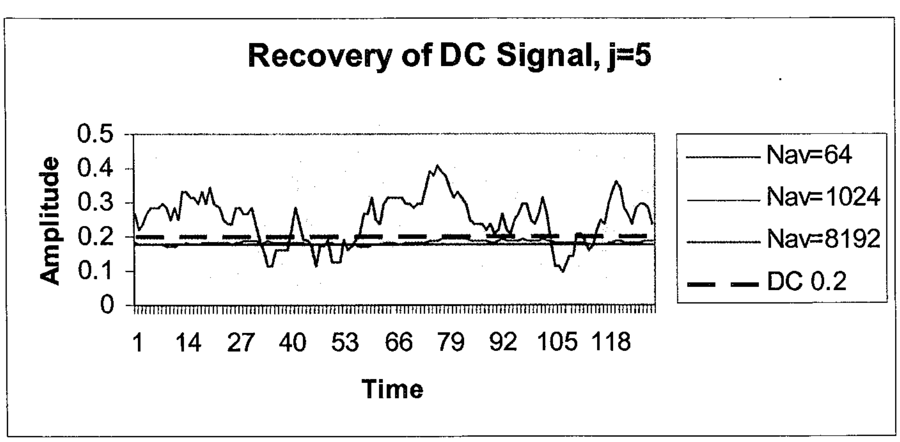

Figure 4.3: Recovery of DC signal for j=5

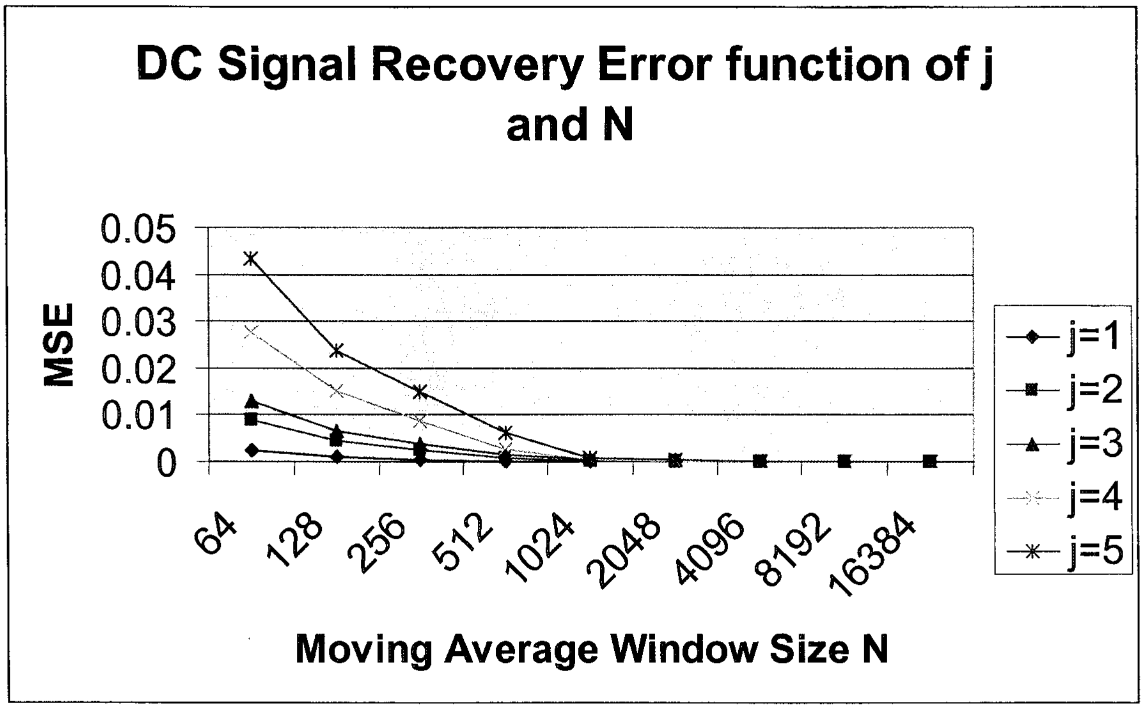

Figure 4.4: DC signal recovery error function of N for some j

4.1.2 Sinusoidal Signal Study

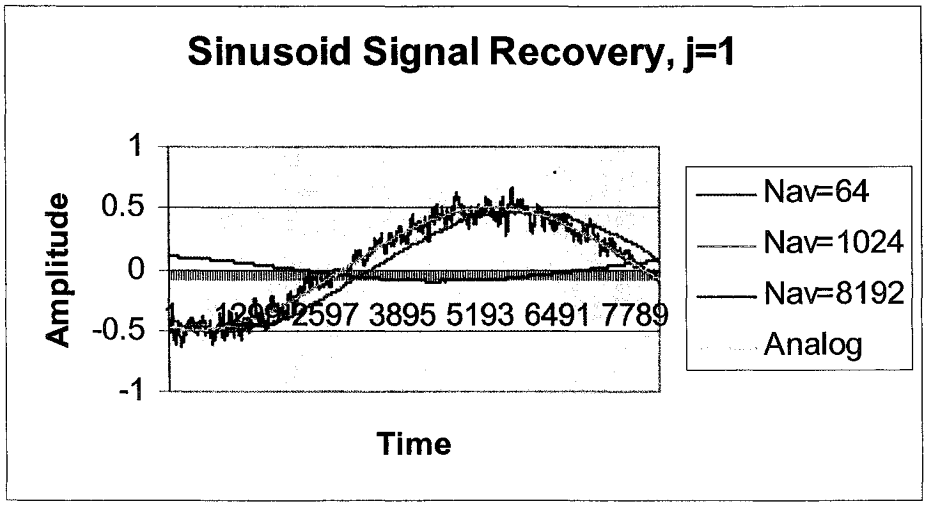

Figure 4.5: Recovery of sinusoid signal for j=1

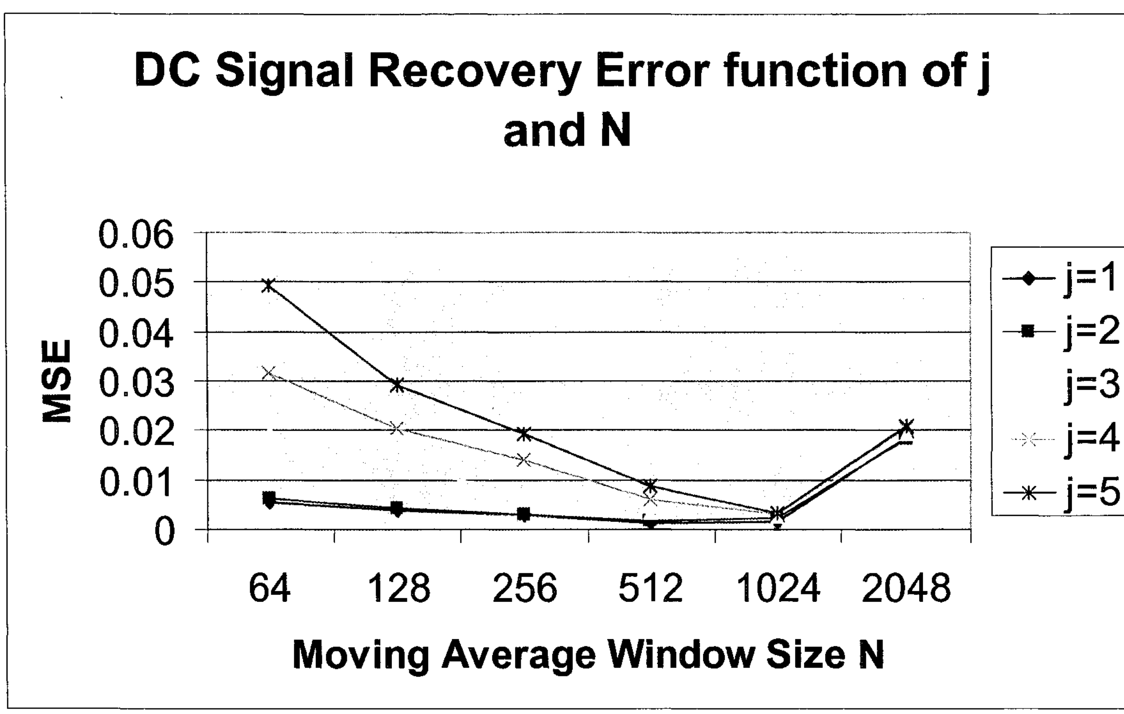

Figure 4.6: Sinusoid signal recovery error function of N for some j

4.1.3 Sin Phase Comp

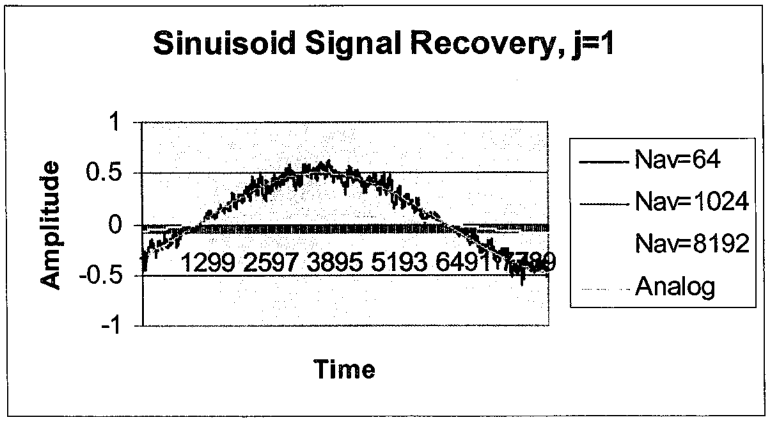

Figure 4.7: Recovery of sinusoid signal with phase compensation for j=1

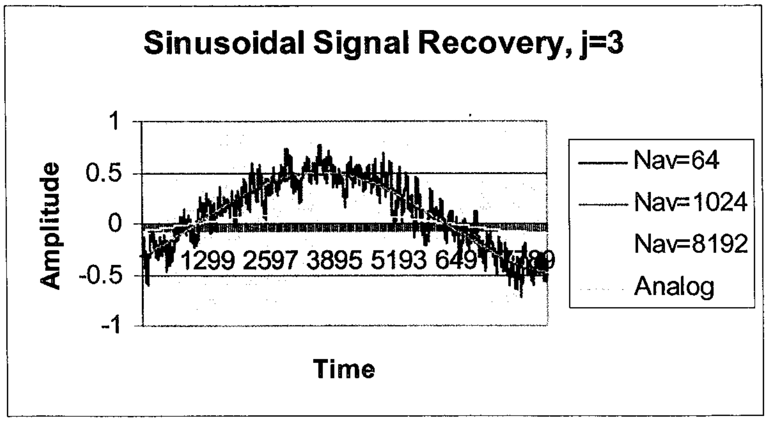

Figure 4.8: Recovery of sinusoid signal with phase compensation for j=3

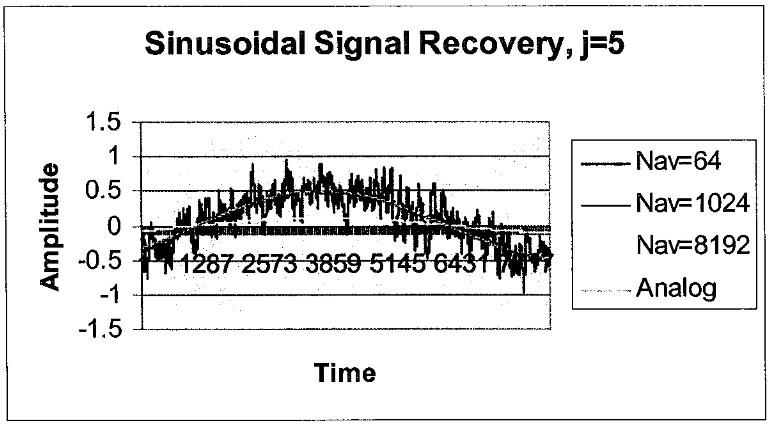

Figure 4.9: Recovery of sinusoid signal with phase compensation for j=1

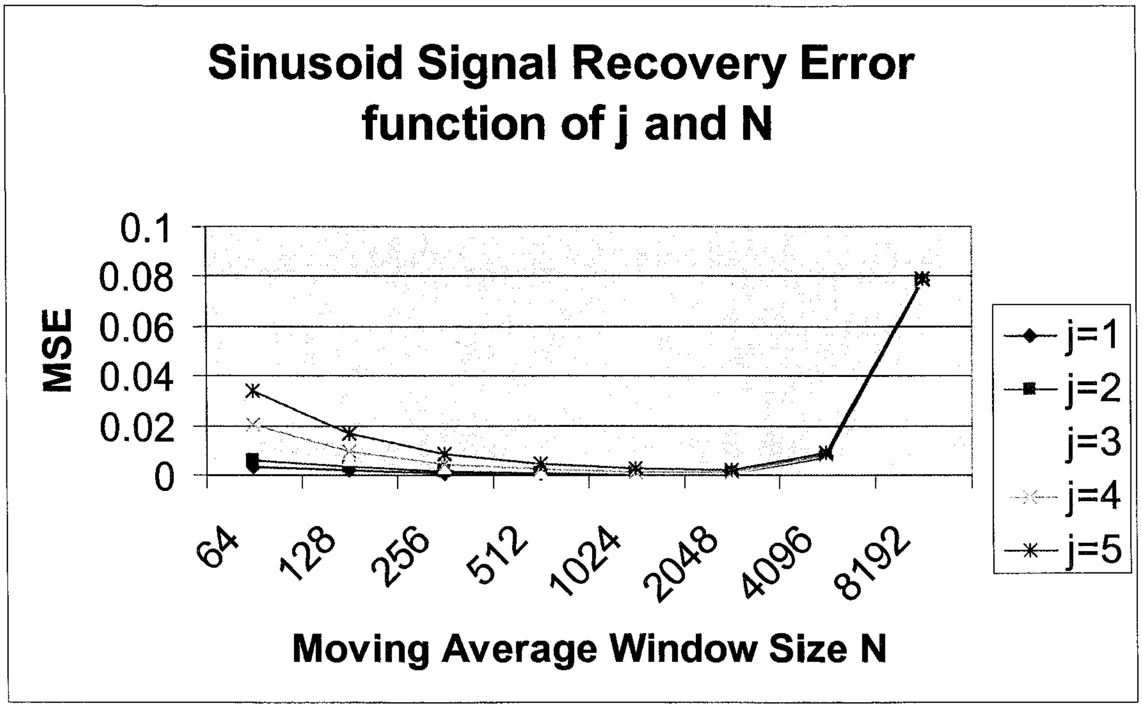

Figure 4.10: Sinusoid signal recovery with phase compensation error function of N for some j

4.1.4 Error for sinusoid recovery for different sinusoid amplitudes

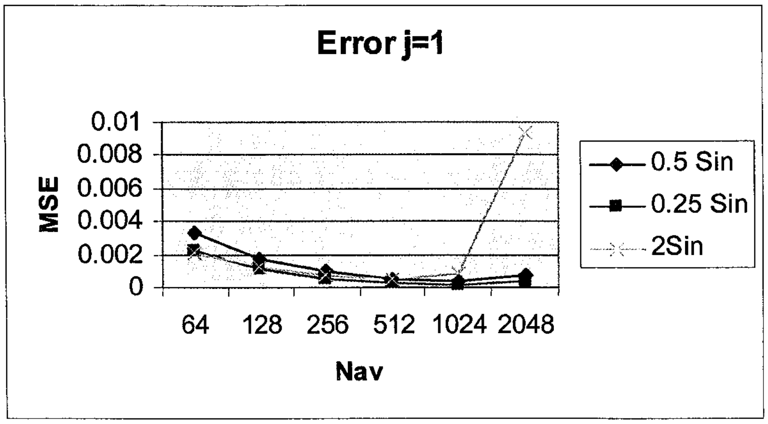

Figure 4.11: Sinusoid signal recovery for different sinusoid amplitudes for j=1

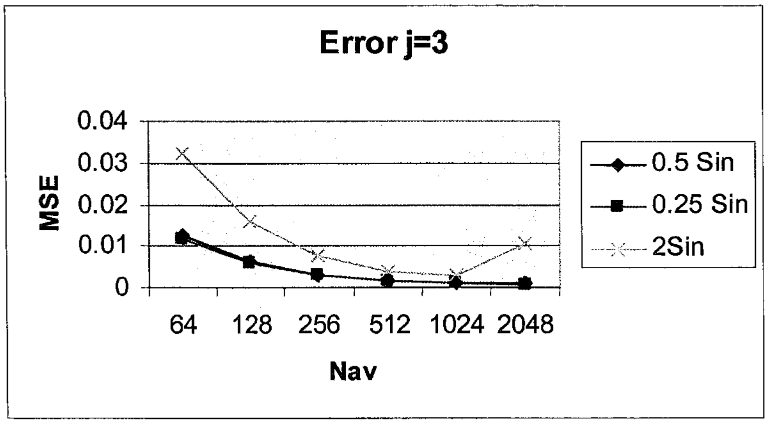

Figure 4.12: Sinusoid signal recovery for different sinusoid amplitudes for j=3

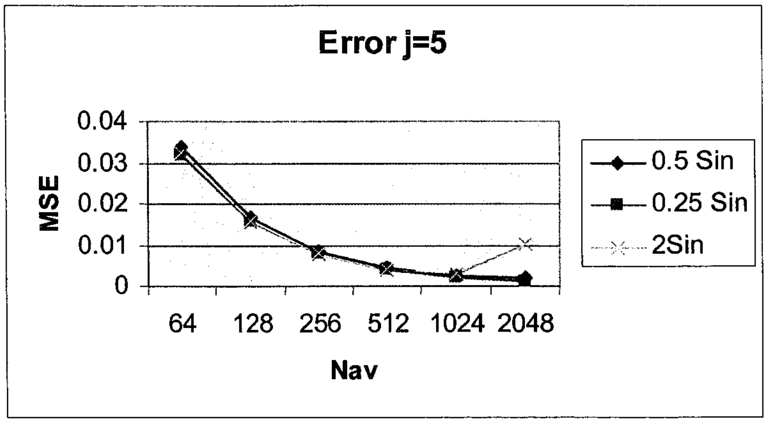

Figure 4.13: Sinusoid signal recovery for different sinusoid amplitudes for j=5

4.2 Experimental Study of RRQ using random noise amplitude domain multiple of (1+d)Δ with d constant or noise

Experimental results using parameters such that $d>0$ and $k.d < 1$ are presented in figure 4.14. The results are consistent with theoretical results predicted in Pop [27].

Testing with d as a uniformly distributed random variable shows a high error level for $j=1$ and smaller error values for $j > 1$, shown in figure 4.15

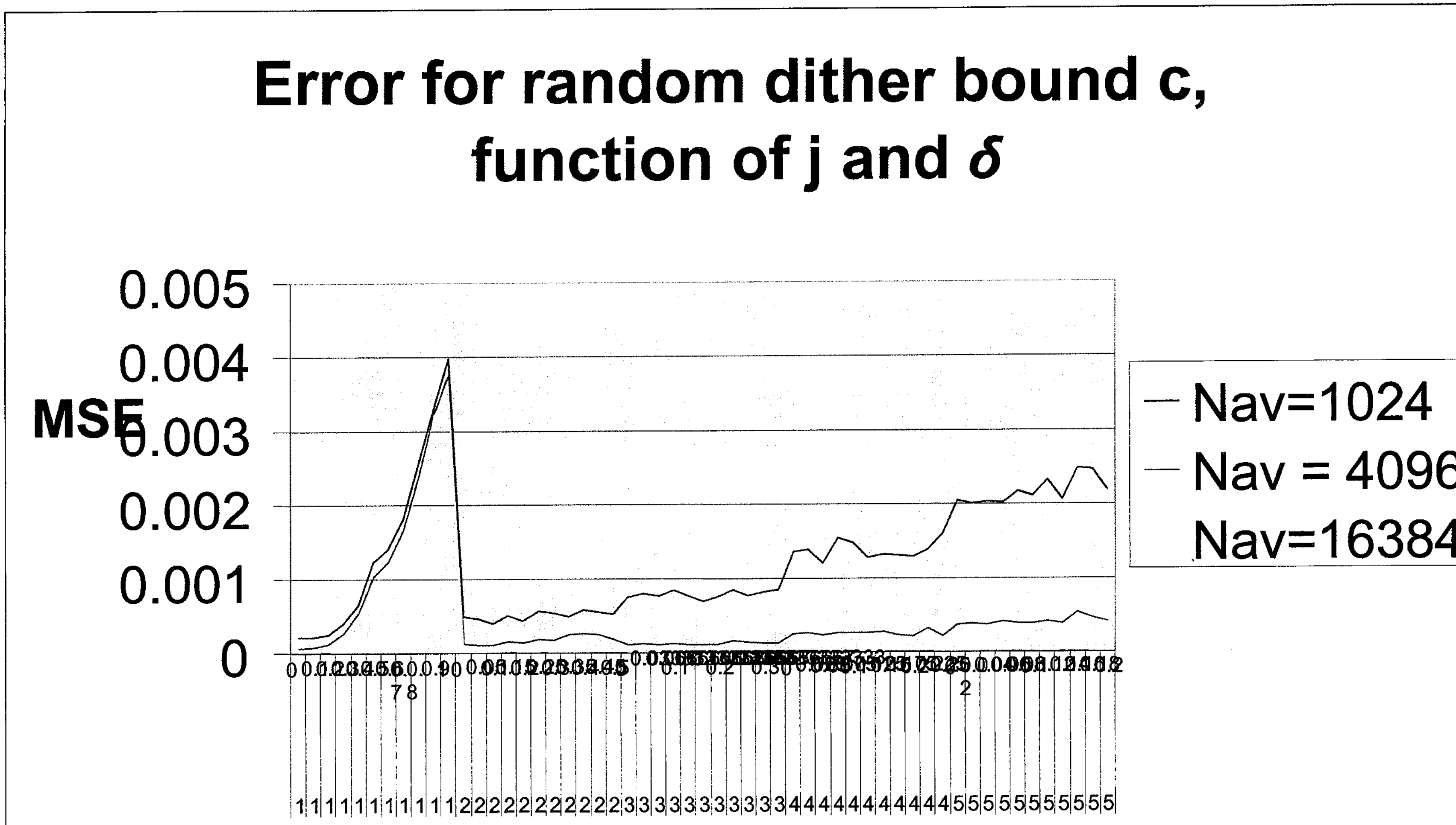

Figure 4.15: Error for random dither bound c, function of j and δ

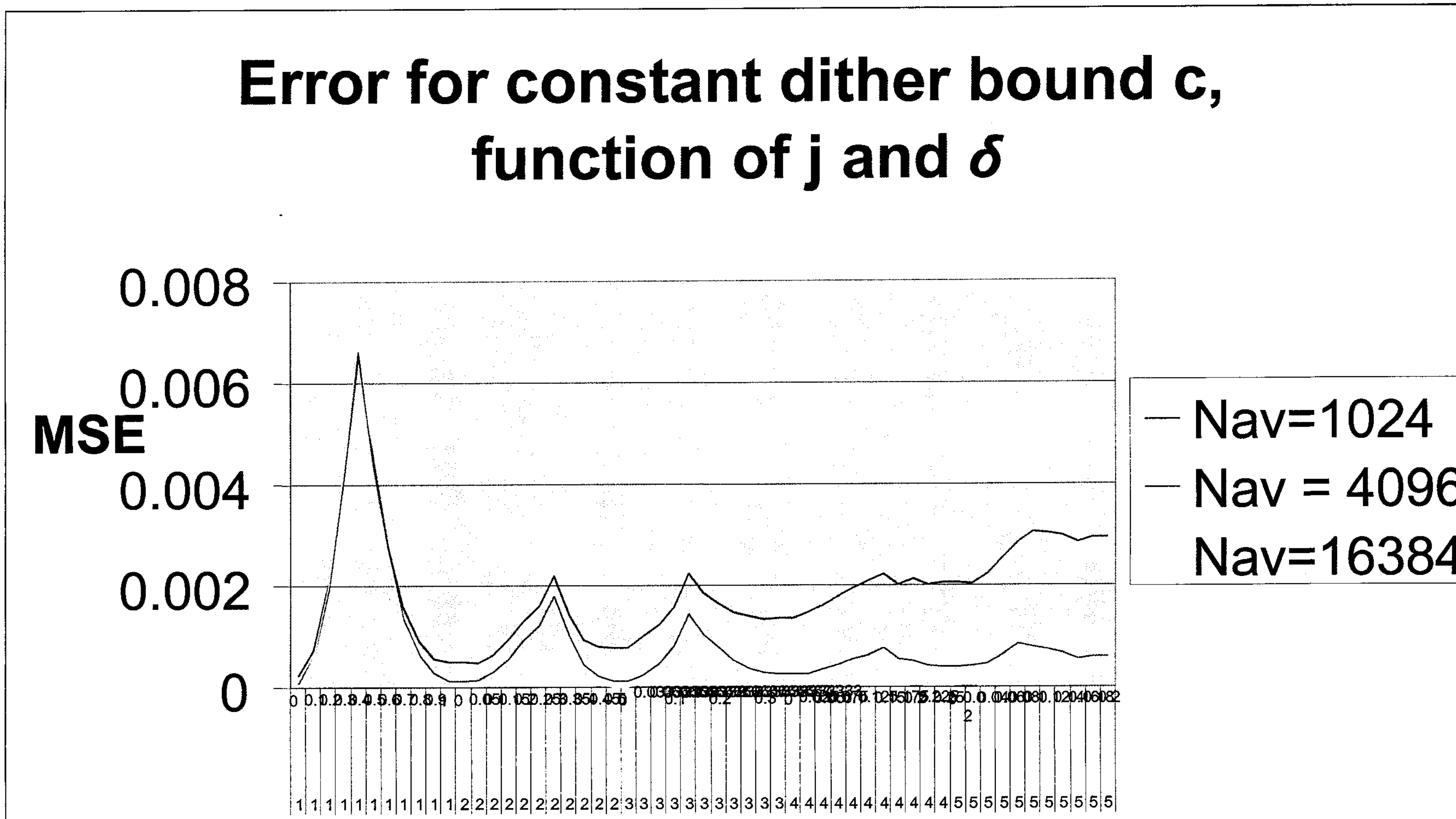

Figure 4.14: Error for constant dither bound c, function of j and δ

4.3 Random Data Multiplication

Figures 4.16 and 4.17 show the MSE observed when performing multiplication in the random-data domain. When multiplying DC signals (Figure 4.16), the error is minimized as the number of samples N_{av} used in averaging increases. Figure 4.17, the error found when multiplying 2 sinusoids, shows similar characteristics to signal recovery of a sinusoid. This should be expected as the multiplication of 2 sinusoids results in another sinusoid.

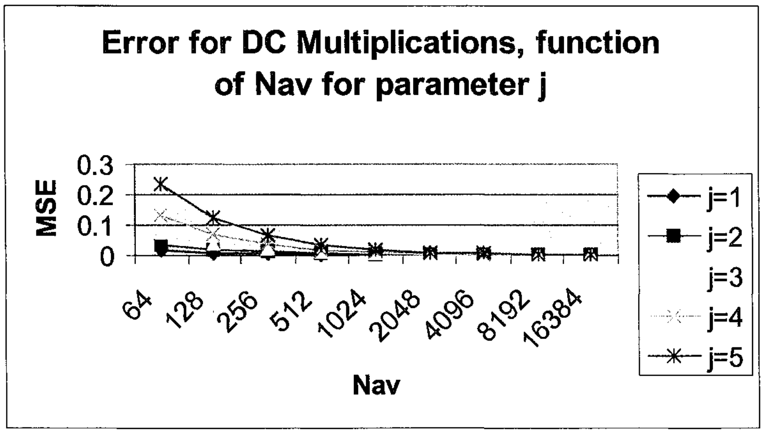

Figure 4.16: Multiplication error for 2 DC signals using random-data representation

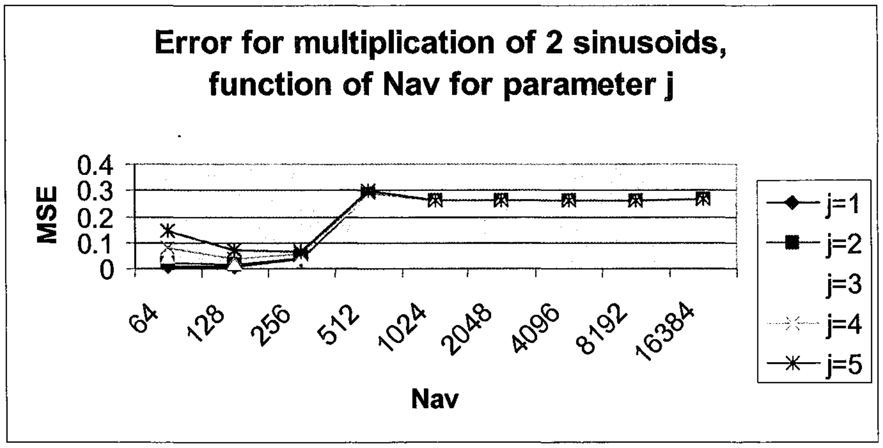

Figure 4.17: Multiplication Error for 2 sinusoidal signals using random-data representation

4.4 Random Data Correlator Output

Correlation diagrams in this chapter show the amplitude of the correlation coefficient plotted against the coefficient index. Figures 4.18, 4.19 and 4.20 show experimental results confirming the proper operation of the random data correlator when used to autocorrelate a sinusoidal input for different values of j. The analytical analog correlation is also show on these graphs to ease visual comparison of the results.

Figure 4.21 demonstrates the correlation function for two sinusoids with a $\pi/2$ phase difference between them. The results are in agreement with the theoretical (analytic) correlation function.

Figure 4.22 shows experimental error values for different dither domains j as a function of the moving average window size N_{av}.

This virtual prototyping environment can be used to simulate calculation of the correlation function for two given inputs. By running for different j and N_{av} parameter values, the most convenient cost-performance architectural trade-off can be chosen.

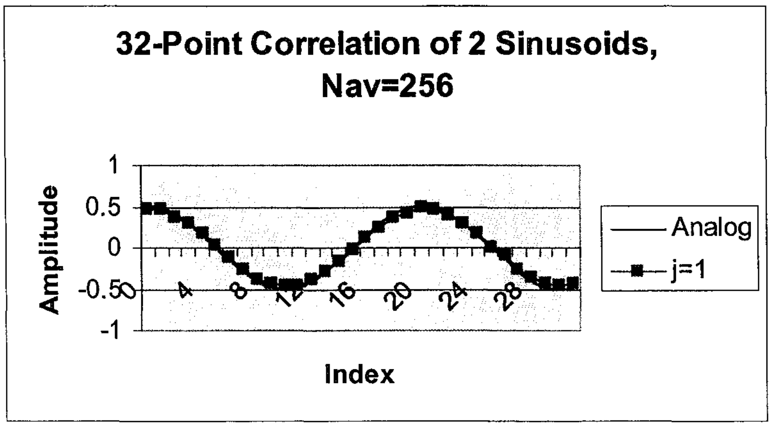

Figure 4.18: 32-point correlation of 2 sinusoids, N_{av}=256, j=1

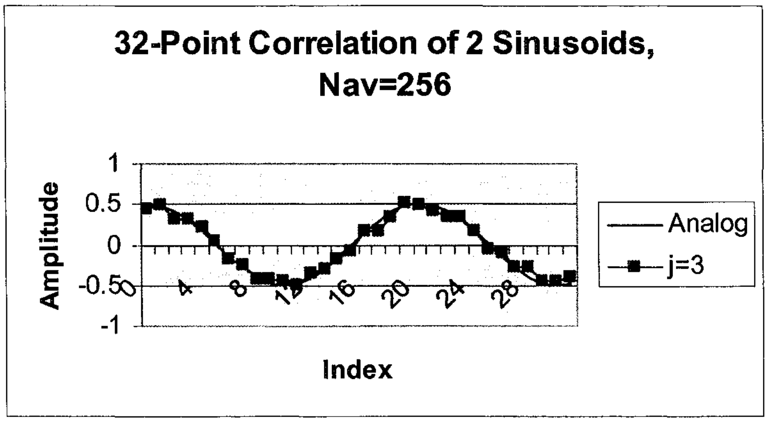

Figure 4.19: 32-point correlation of 2 sinusoids, N_{av}=256, j=3

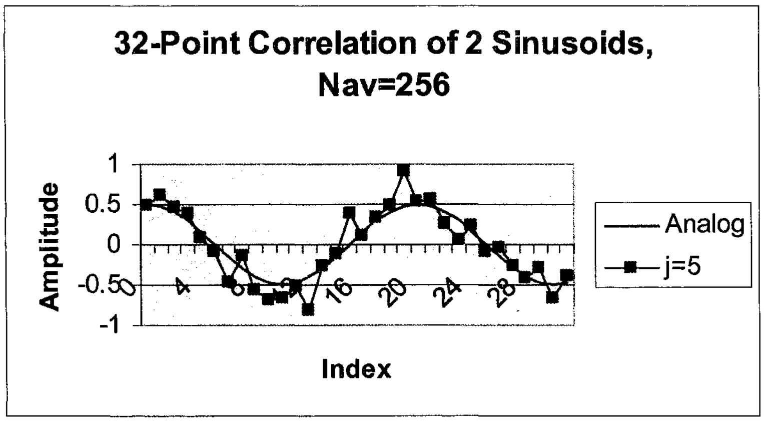

Figure 4.20: 32-point correlation of 2 sinusoids, N_{av}=256, j=5

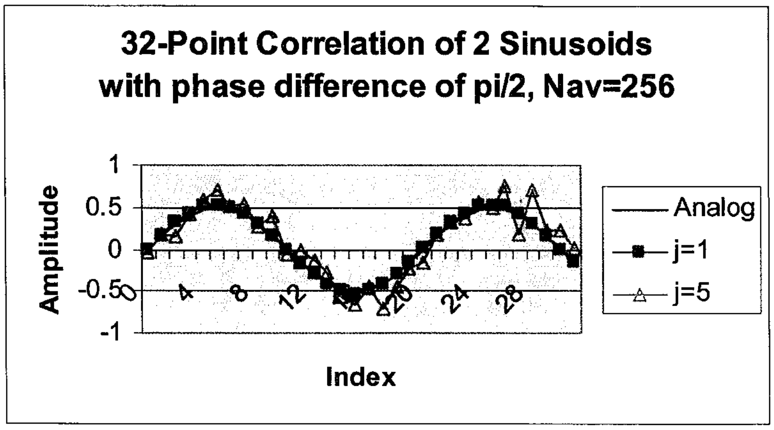

Figure 4.21: 32-point correlation of 2 sinusoids with phase difference of $\pi/2$, N_{av}=256, j=1 and j=5

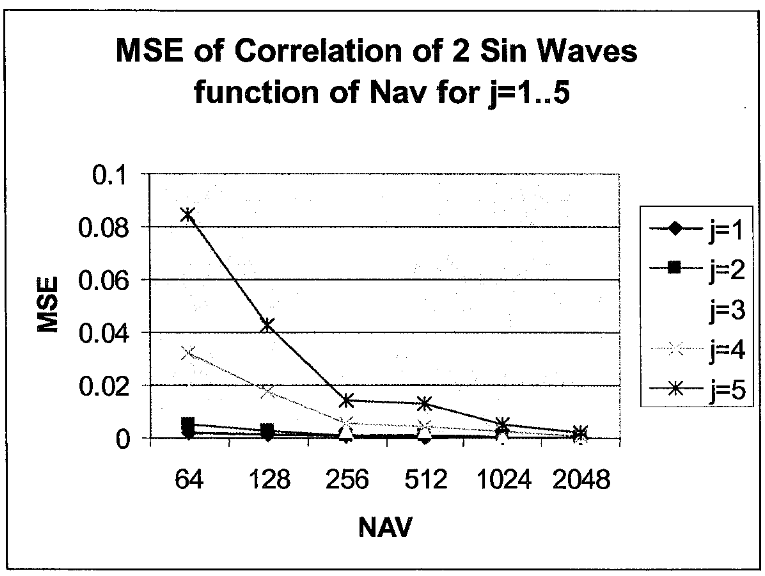

Figure 4.22: MSE of correlation function of 2 sin waves function of N_{av} for j=1..5

Chapter 5: Conclusion

5.1 Conclusion

The research produced a virtual prototyping environment to study generalized random data based systems. The VPE evaluates the error performance of random data conversion, multiplication, and correlation with respect to a variety of input signals and system parameters.

In the process, experimental results on the effects of having an error δ in the random reference quantization were studied for constant and randomly distributed values.

5.2 Further research

Further research into the effects of the reference domain instability of the dither signal can be accomplished by modifying the δ signal in the experiments. Hardware models estimating speed of operation and hardware implementation costs can be investigated once acceptable operating parameters for error requirements have been determined using the VPE designed in this work.

Bibliograpy

[1] Al-Dhaher, A., Petriu, E.M., Dostaler, M., "FPGA Correlator Architecture Using Random-Pulse Data Representation", *Proceedings of the 19th IEEE Instrumentation and Measurement Technology Conference,*vol.2, pp1061-1063, May 2002

[2] Alspector, J., Gannett, J.W., Haber, S., Parker, M.B., Chu, R., "Generating Multiple analog noise sources from a single Linear Feedback Shift Register with Nerual Network Applications", *IEEE Symposium on Circuits and Systems*, vol.2, pp.1058-1061, May 1990

[3] Alspector, Gannett, Haber, Parker, Chu, "A VLSI-Efficient Technique for Generating Multiple Uncorrelated Noise Sources and its Application to Stochastic Neural Networks", *IEEE Transactions on Circuits and Systems*, vol.38, no.1, pp109-122, January 1991

[4] Astaras, A., Dalzell, R., Murray, A., Reekie, M., "Pulse Based Circuits and Methods for Probabilistic Neural Computation", *Proceedings of the Seventh International Conference on Microelectronics for Neural, Fuzzy and Bio-Inspired Systems*, pp96-102, April 1999

[5] Bade, Hutchins, "FPGA-Based Stochastic Neural Networks – Implementation", *IEEE Workshop on FPGAs for Custom Computing Machines Workshop*, Napa, CA, pp189-198, April 10-13, 1994

[6] Berndt, H., "Correlation Function Estimation by a Polarity Method Using Stochastic Reference Signals", *IEEE Transactions on Information Theory*, vol.14, no.6, pp.796-801, November 1968

[7] Castanie, F., "Signal Processing by Random Reference Quantizing", *Signal Processing*, pp.27-43, 1979

[8] Castanie, F., Hoffmann, J.C., Lacaze, B., "On the Performance of a Random Reference Correlator", *IEEE Transactions on Information Theory*, vol.20, no.2, pp266-269, March 1974

[9] Carbone, P., Caciotta, M., "Stochastic-Flash Analog-to-Digital Conversion", IEEE Transactions on Instrumentation and Measurement, vol.47, no.1, pp.65-68, February 1998

[10] Carbone, P., Petri, D., "Effect of Additive Dither on the Resolution of Ideal Quantizers", IEEE *Transactions on Instrumentation and Measurement*, vol.43, no.3, pp.389-396, June 1994

[11] Carbone, P., Petri, D. "Performance of Stochastic and Deterministic Dithered Quantizers", *IEEE Instrumentation and Measurement*, vol.49, no.2, pp.337-340, April

2000

[12] Chang, K.Y., Moore, D., "Modified Digital Correlator and Its Estimation Errors", *IEEE Transactions in Information Theory*, Vol.IT-16, no.6, pp.699-706, November, 1970

[13] Dostaler, M.; Petriu, E.M.; Al-Dhaher, A.H.; Groza, V.Z., "Parallel Correlator Architecture for Real-Time Sensing Applications", *2nd ISA/IEEE Sensors for Industry Conference*, pp180-185, 19-21 November 2002

[14] Florek, A., Kozlowski, K., Wroblewski, W., Gapinski, J., "Personal Computer-Controlled Digital Correlator", *Journal of Microcomputer Applications*, no.14, pp27-37, 1991

[15] Florek, A., Kozlowski, K., Wroblewski, W., Gapinski, J., "Computer-controlled Digital Correlator and its application in Experimental Physics", *Microprocessors and Microsystems*, Vol.16, no.4, pp171-176, 1992

[16] Gaines, B.R., "Stochastic Computer Thrives on Noise", *Electronics Letters*, pp.72-79, July 1967

[17] Gray, R., Stockham, T., "Dithered Quantizers", *IEEE Transactions on Information Theory*, vol.39, no.3, pp.805-812, May 1993

[18] Halimi, M., Castanie, F., "A Comparison of Several Optimal Random Quantization Algorithms for Correlation Estimation", *IEEE International Conference on Acoustics, Speech and Signal Processing*, vol.9, pp542-545, 1984

[19] Jespers, P., Chu, P.T., and Fetweis, A., "A New Method to Computer Correlation Functions", in *Intl. Symposium on Information Theory*, Brussels, Belgium, 1962

[20] Miller, A.J., Brown, A.W., and Mars, P., "Moving Average Output Interface for Digital Stochastic Computers", *Electronics Letters*, vol.10, no. 20, pp.419-420, October 1974

[21] von Neuman, J, "Probabilistic logics and the synthesis of reliable organisms from unreliable components," in *Automata Studies,* (CE Shannon, Ed.), Princeton, NJ, Princeton University press, 1956

[22] Padin, S.; Clark, T.S.; Ewing, M.S.; Finch, R.P.; Lawrence, R.P.; Navarro, J.; Scott, S.L.; Scoville, N.Z.; Seelinger, C.; Seling, T.V.; "A high-speed digital correlator for radio astronomy", *IEEE Transactions on Instrumentation and Measurement*, vol.42 , no.4, pp.793–798, August 1993

[23] Petriu, E.M., Al-Dhaher, A., Zhao, L., Dostaler, M., "Modular Architecture for Statistical Signal Parameter Measurement Using Multi-bit Random-Data

Representation", *IEEE Pacific Rim Conference on Communications, Computers and Signal Processing*, vol.1, pp295-298, 26-28 August 2001

[24] Petriu, E.M., Gendron, S., "Ramp-Type Analog-to-Digital Conversion as 1-bit Dithered Quantization", *Canadian Conference on Electrical and Computer Engineering, Ottawa, ON*, Sep3-6, 1990

[25] Petriu, E., Watanabe, K., Yeap, T., "Applications of Random-Pulse Machine Concept to Neural Network Design", IEEE Transactions on Instrumentation and Measurement, vol.45, no.2, pp.665-669, 1996

[26] Petriu, E.M., Zhao, L., Das, S.R., Groza, V., Cornell, A., "Instrumentation Applications of Multi-bit Random-Data Representation", *IEEE Transactions on Instrumentation and Measurement*, vol.52, no.1, February 2003

[27] Pop, E., Petriu, E.M., "Influence of Reference Domain Unstability Upon the Precision of Random Reference Quantizer with Uniformly Distributed Auxiliary Source", *Signal Processing* (EURASIP), North Holland, Vol. 5, pp.87-96, 1983.

[28] Poppelbaum, W.J. and Afuso, C., "Noise-Computer," *University of Illinois, Urbana, Dept. Comp Sc., Quarterly Technical Progress Reports*, January-March 1965, July-September 1965, January-March 1966

[29] Ribeiro, S.T., "Random-Pulse Machines", *IEEE Transactions on Electronic Computers*, vol EC-16, no. 3, pp.261-276, June 1967

[30] Roberts, L.W., "Picture Coding Using Pseudo-Random Noise", *IRE Transactions on Information Theory*, vol, IT-8, pp.145-154, February 1962

[31] Salapura, V., Gschwing, M, Maischberger, O., "A Fast FPGA Implementation of a General Purpose Neuron", *Field-Programmable Logic: Architectures, Synthesis and Applications*, Springer-Verlag, Berlin, pp.175-182, 1994

[32] Schuchman, L., "Dither Signals and Their Effect on Quantization Noise", *IEEE Transactions on Communication Technology*, vol.12, pp162-165, December 1964

[33] Vanderkooy, "Resolution Below the Least Significant Bit in Digital Systems with Dither", Journal of Audio Engineering Society, vol.32, pp106-113, November 1984

[34] Vanderkooy, Lipshitz, "Dither in Digital Audio", Journal of Audio Engineering Society, vol.32, no.3, December 1987

[35] Wagdy, M.F., "Effect of Various Dither Forms on Quantization Errors of Ideal A/D Converters", *IEEE Transactions on Instrumentation and Measurement*, vol.38, no.4, pp850-855, August 1989

[36] Wagdy, M.F. and Goff, M., "Linearizing Average Transfer Characteristics of Ideal ADC's via Analog and Digital Dither", *IEEE Transactions on Instrumentation and Measurement*, vol.43, no.2, pp146-150, April 1994

[37] Wagdy, M.F., and Ng, W., "Validity of Uniform Quantization Error Model for Sinusoidal Signals Without and With Dither", *IEEE Transactions on Instrumentation and Measurement*, vol.38, no.3, pp.718-722, June 1989

[38] Wannamaker, R.A.; Lipshitz, S.P.; Vanderkooy, J.; Wright, J.N., "A theory of nonsubtractive Dither", *IEEE Transactions on Signal Processing*, vol.48 , no.2, pp.499-516, February 2000

[39] Welffenbuttel, R., Kurniawan, W., "Stochastic Analog-to-Digital Converter Based on the Asynchronous Sampling of a Reference Triangle", *IEEE Transactions on Instrumentation and Measurement*, vol.38, no.1, pp. 10-16, February 1989

[40] White & Pickup, "Systematic Errors in Cross Correlation", IEEE Transactions on Instrumentation and Measurement, vol.36, pp47-53, March 1987

[41] Widrow, B., "A Study of Rough Amplitude Quantization by Means of Nyquist Sampling Theory", *IRE Transacations on Circuit Theory,* vol. CT-3, pp.266-276,December 1956

[42] Wolff, S.S., Thomas, J.B., Williams, T.R., "The Polarity Coincidence Correlator: A Nonparametric Detection Device", *IRE Transactions on Information Theory*, pp5-9, January 1962

[43] Yeap, Vokovitch, Eatherly, Petriu, "Neural Network Architecture using Random-Pulse Data Processing", International *Symposium on Circuits and Systems*, vol.3, pp2185-2188, 28 April-3 May 1995

[44] Zhao, L., "Random Pulse Artificial Neural Network Architecture", MASc Thesis, University of Ottawa, ON, Canada, 1998

APPENDIX A – Moving Average/ARMA Frequency Response

In this research, the term "relatively slow varying rate signal" is employed without specifying what constitutes "relatively slow". The signal is relatively slow compared to the system's sampling rate, but again no value is given. In an effort to define acceptable values, a quick analysis of the random-data/data conversion algorithm is performed.

The Random Data/Digital conversion is an average taken over a finite number of samples N. As an FIR filter, the equation is

$$y[n] = \sum_{n=0}^{M-1} x(n) \tag{A.1}$$

In order to reduce the computation time for each output, the Random Data/Digital conversion is implemented as a moving average algorithm. Given a filter of length M,

$$y[n] = y[n-1] + \frac{1}{M}\left(x(n) - x(n-(M-1))\right) \tag{A.2}$$

Using the Z-Transform, the transfer function is determined

$$\begin{aligned} Y(z) &= Y(z)z^{-1} + \frac{1}{M}(X(z) - X(z)z^{-(M-1)}) \\ Y(z)(1-z^{-1}) &= X(z)\left(\frac{1}{M} - \frac{z^{-(M-1)}}{M}\right) \\ H(z) &= \frac{Y(z)}{X(z)} = \frac{1}{M} \bullet \frac{1-z^{-(M-1)}}{1-z^{-1}} \end{aligned} \tag{A.3}$$

A.1 Magnitude Response

The magnitude response is computed as follows

$$|H(z)| = \left| \frac{1}{M} \left[\frac{1 - z^{-(M-1)}}{1 - z^{-1}} \right] \right|$$

$$|H(z)| = \left| \frac{2}{M(1 - z^{-1})(1 + z^{-(M-1)})} \left[\frac{z^{\frac{(M-1)}{2}} - z^{-\frac{(M-1)}{2}}}{2} \right] \right| \qquad \text{(A.4)}$$

The following graph shows the frequency response for M values of 8 (blue), 16 (red), 32 (green) and 64 (yellow).

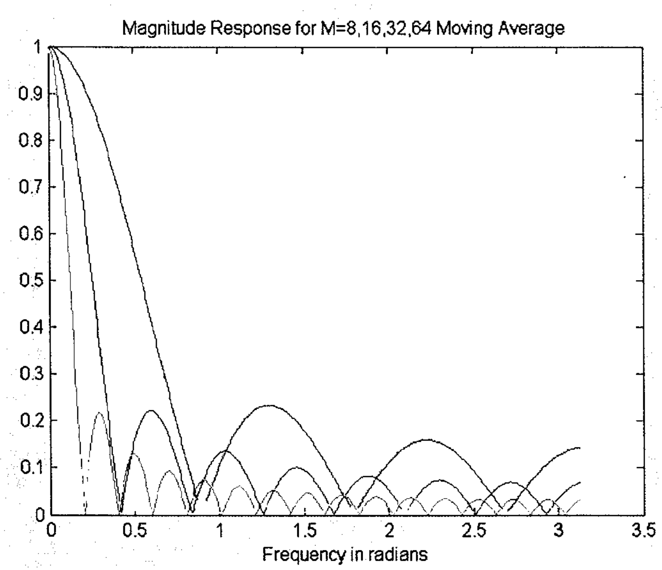

The moving average is in effect a low pass filter, with a narrow passband. The simplicity in the implementation has as a tradeoff a poor rolloff characteristic and poor attenuation in the stop band. Since the goal is to convert the random data stream to its digital representation, the rolloff and attenuation are of lesser concern; it is the passband that needs to be examined.

A.2 Phase Response

The phase response for the moving average filter is linear. The case of a M=8 moving average is shown below

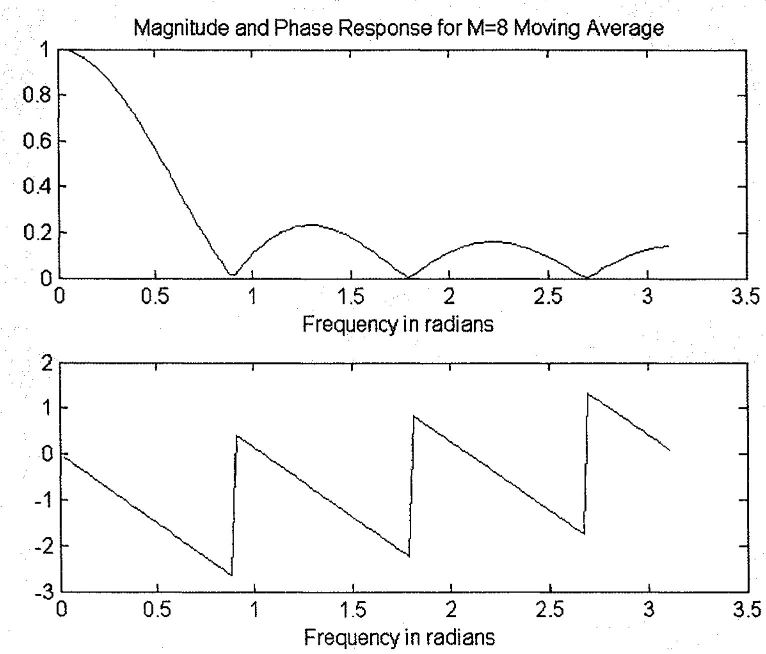

With respect to the cross-correlation being calculated in this work, the signals of interest have the same frequencies and thus the phase shift is identical for them. If the frequencies of the signals being processed in such a system are not identical, the phase shifts need to be taken into account or corrected using additional signal conditioning.